Gravity and magnetic modelling along seismic reflection profiles across the East Shetland Platform (Northern North Sea, UK)

Mattia De Luca[1], Paolo Mancinelli[1], Stefano Patruno[2], Vittorio Scisciani[1]

[1]Department of Engineering and Geology, G. d'Annunzio University of Chieti-Pescara, Italy

[2]Department of Engineering, University of Nicosia, Cyprus

Engineering and Geology Department

"G. d'Annunzio" University of Chieti-Pescara

EGU General Assembly #EGU23 23 - 28 April 2023

This presentation participates in OSPP

Outstanding Student & PhD candidate Presentation contest

Sharing is encouraged

TAP TO NAVIGATE

ABSTRACT

TAP TO NAVIGATE

AREA OF INTEREST

- GEOLOGICAL SETTING
- BASEMENT
- STRATIGRAPHY

DATA

- BOREHOLE
- SEISMIC
- MOHO DEPTH
- POTENTIAL FIELDS
  - FILTERING
- GEOTHERMAL GRADIENT

DATA SUMMARY

METHODS

RESULTS

- SECTION A
- SECTION B
- SECTION C
- SECTION D
- SECTION E
- SECTION F

SEISMIC VS. GRAVITY

BASINS THICKNESS

HIGH-SUSCEPTIBILITY SOURCES

CONCLUSIONS

FUTURE STEPS

MANUSCRIPT SUBMITTED TO TECTONOPHYSICS

REFERENCES

EGU General Assembly #EGU23 23 - 28 April 2023

This presentation participates in OSPP — Outstanding Student & PhD candidate Presentation contest

Sharing is encouraged

Ud'A Università degli Studi "G. d'Annunzio"

INGEO

TITLE SLIDE

AREA OF INTEREST

…why this area?

- Underexplored area
- Uncertain geological framework
- Debated geodynamic evolution
- Data availability

AREA OF INTEREST – Framework

- 33,000 Km^2
- Proximity to triple rift-zone
- Permo-Triassic and mid-Devonian basins
- Tectonic highs with shallow acoustic basement and rare mature source rocks
- Field evidence of gabbroic and serpentinized rocks

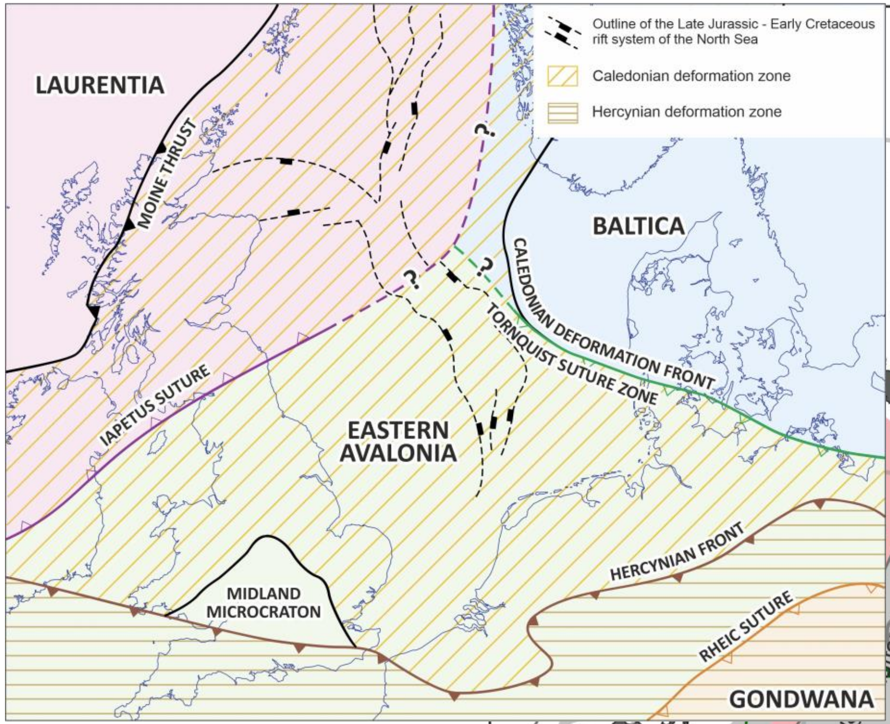

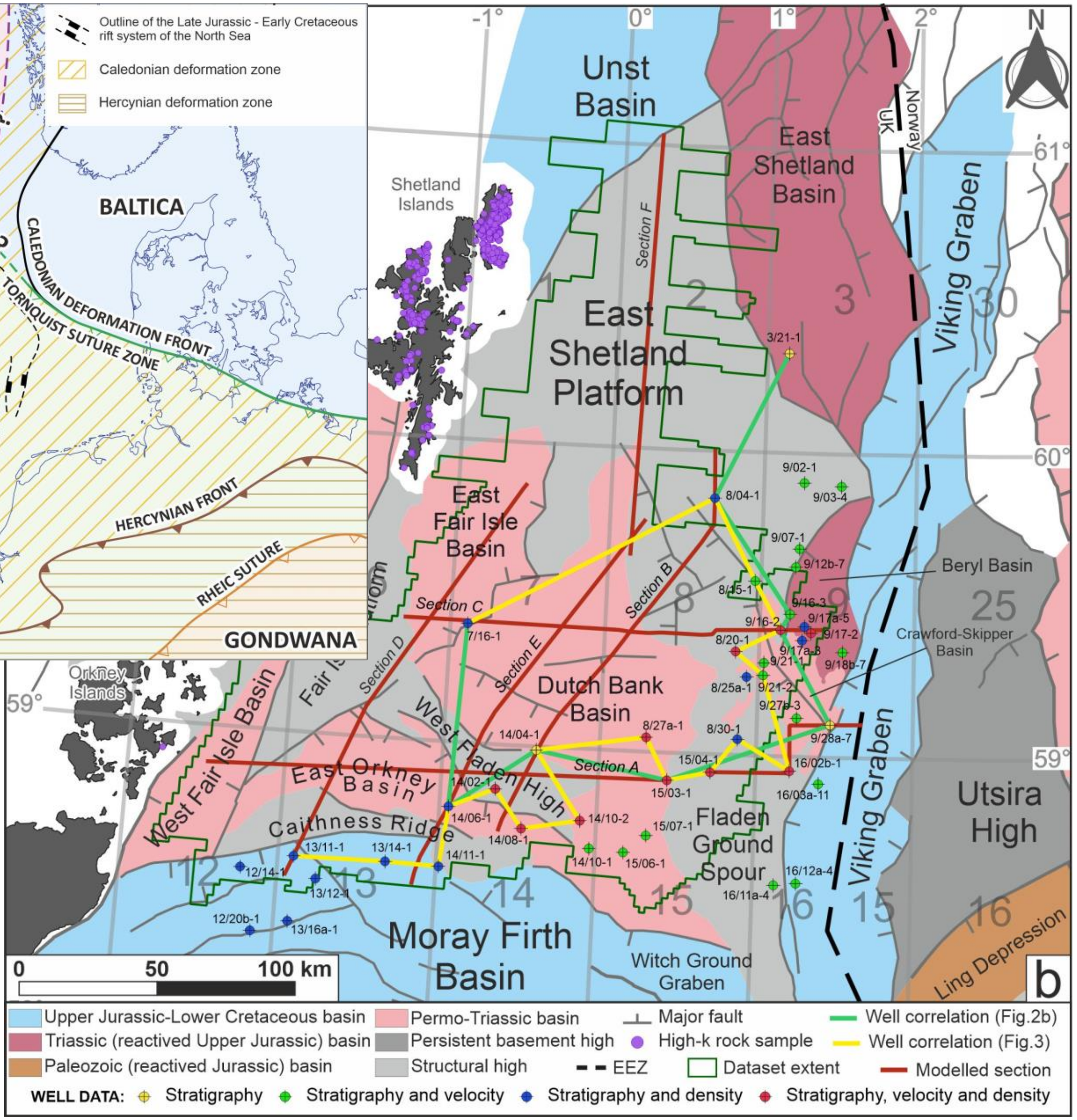

(Above) Regional tectonic setting of North Sea (modified from Zanella et al., 2003). (Right) Area of Interest (AOI) structural scheme showing the main Paleozoic-Mesozoic basins and structural highs in the Northern North Sea (NNS) modified from Scisciani et al. (2021). Dataset extent indicates Bouguer gravity and magnetic anomaly data from Bliss et al. (2016). Traces of seismic lines and geological cross-sections modelled in this work are in red; seismic profiles were retrieved from the National Data Repository (NSTA, 2022). Violet dots show the distribution of onshore gabbroic, serpentinite and serpentinized rock samples (BGS, 2022).

STRATIGRAPHY

Greater East Shetland Platform – LITHOLOGIES

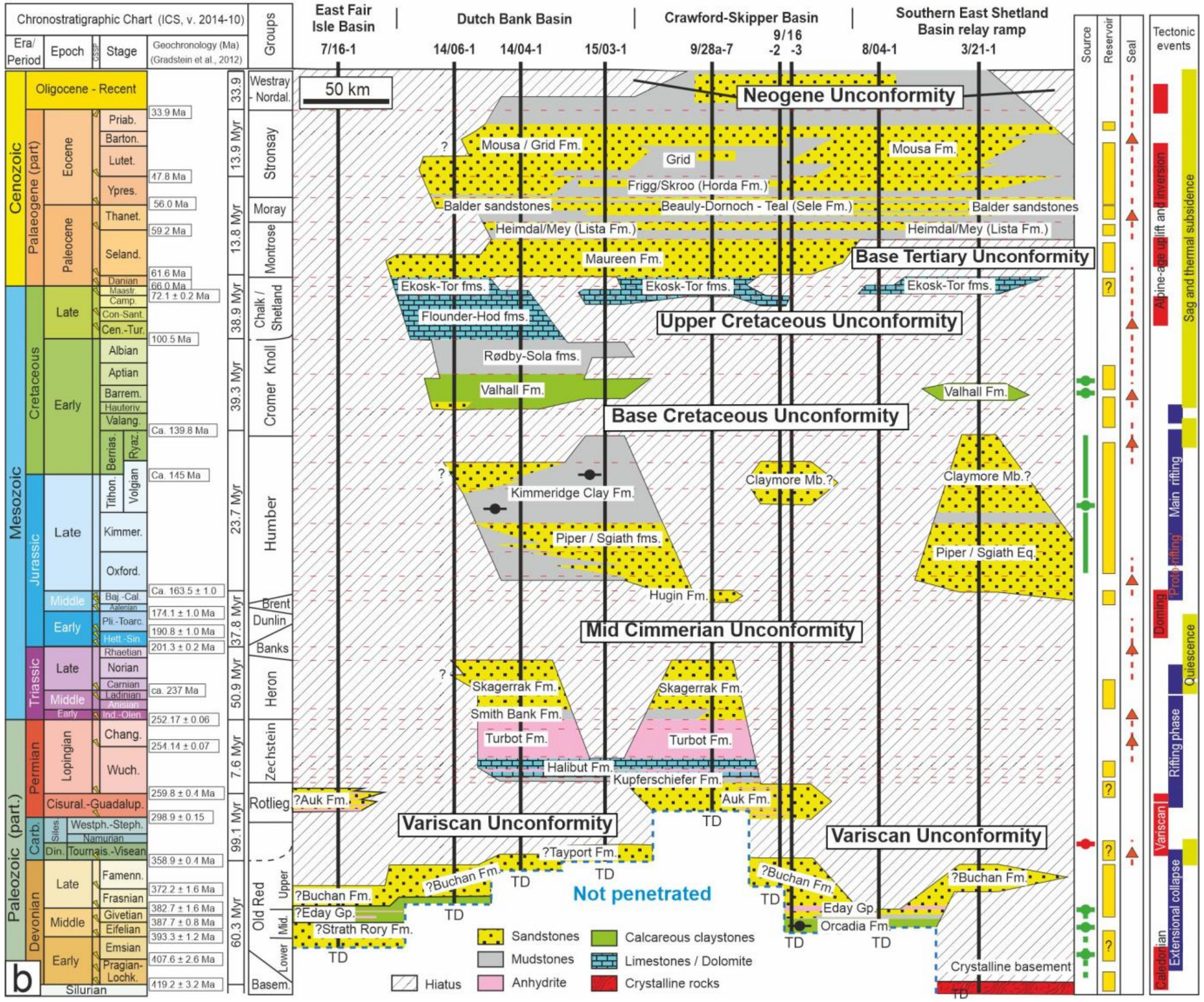

- Paleocene to Recent: Sandstone and Mudstone/Shale
- Upper Cretaceous: Limestone
- **Lower Cretaceous**: Mudstone/Shale/Marls
- **Jurassic and Triassic**: Mudstone/Shale and Sandstone
- Upper Permian: Anhydrite, Limestone, Dolomite
- Lower Permian: Sandstone
- Devonian: Sandstone and Marls
- Pre-Devonian: **Crystalline Basement**

(Left) Regional chronostratigraphic and lithostratigraphic correlation panel of wells (green line in AOI figure) showing the inhomogeneous lateral and vertical distribution of the sedimentary cover and unconformities related to the main tectono-magmatic events (modified from Scisciani et al., 2021) . **(Below)** Regional well-correlation panel (yellow line in AOI figure).

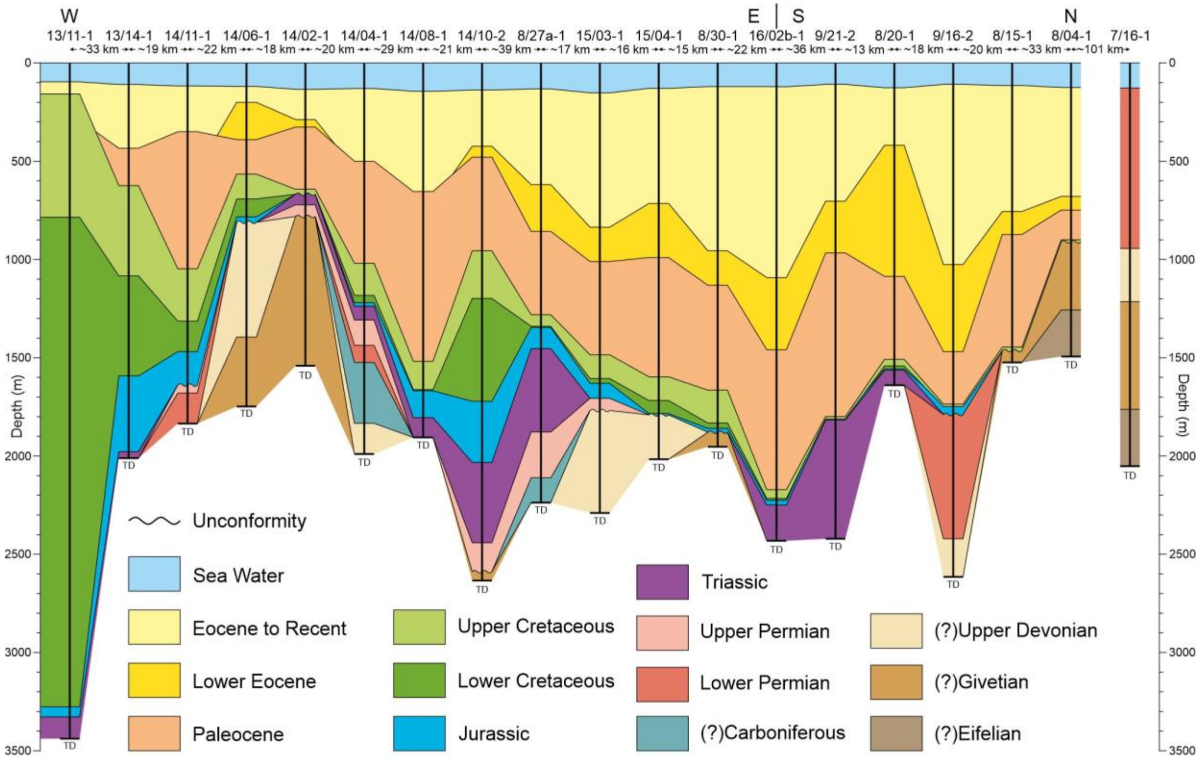

PRE-DEVONIAN BASEMENT

Basement composition from Bassett (2003)

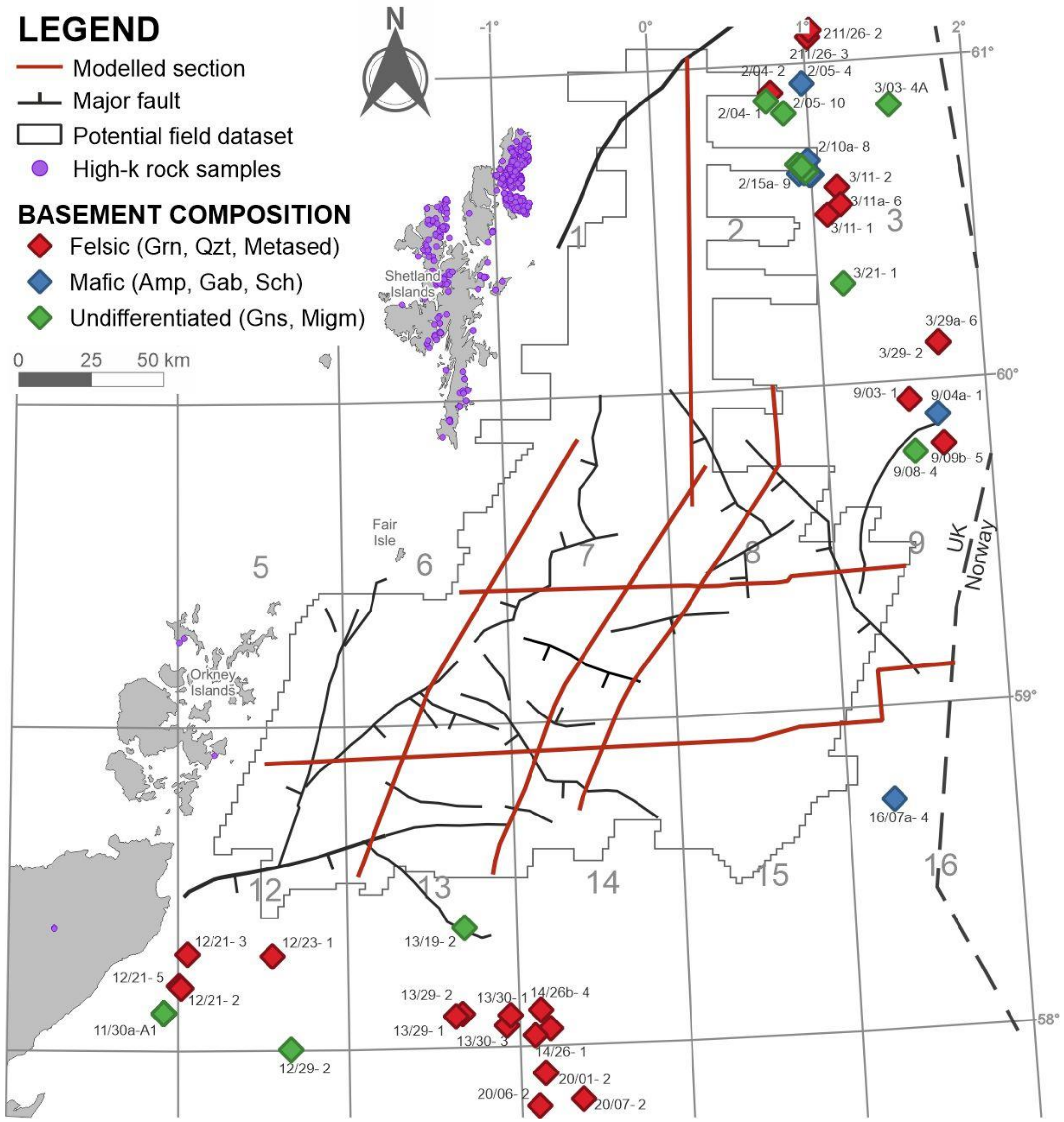

WHAT WE KNOW ON THE GEOLOGY OF THE BASEMENT?

- **Poorly investigated** within and around the AOI
- **Drilled** and **sampled** only its **shallowest part**
- Prevalent composition: **granite** and **metasedimentary rocks**
- **Field evidence of gabbroic and serpentinized rocks**

PETROPHYSICS OF SURROUNDING WELL CORES (from Fichler et al., 2011)

Ref.	Well	Country	Lithology	Geochronologic age (Ma)	Susceptibility [10^{-6}SI]	Remanence (10^{-3} Am^{-1})	Density [g/cm^3]
1b	36/1-1	N	Granitic gneiss		104	5.2	2.676
2b	35/3-4	N	Biotite gneiss		234	0	2.773
3b	35/9-1	N	Breccia		286	0	2.619
4b	25/11-17	N	Metasiltstone		292	0	2.656
5bc	16/1-4	N	Leucogabbro	421	448.4	32.1	2.765
6b	17/3-1	N	Breccia		300	5	2.71
7a	16/2-1	N	Biotite microgranite	446 [1]; 409[6]			
8bc	16/3-2	N	Granite	456	949.7	48.8	2.680
9bc	16/4-1	N	Granite	460	88	6.9	2.646
10bc	16/5-1	N	Granite	463	179.8	11.3	2.662
11abc	16/6-1	N	Porphyric volcanic rock	447 [45]; 430	181.1	9.5	2.591
12a	210/4-1	UK	Biotite gneiss	442 [2]			
13a	BGS81/17	UK	Hornblendite	697 [13]			
14a	211/26-1	UK	Biotite–garnet gneiss, greenschist	430			
15a	9/4-1	UK	Hornblendebiotite schist	393 [7]			

a—Bassett (2003), b—Slagstad et al. (2008), c—Slagstad et al. (2011).

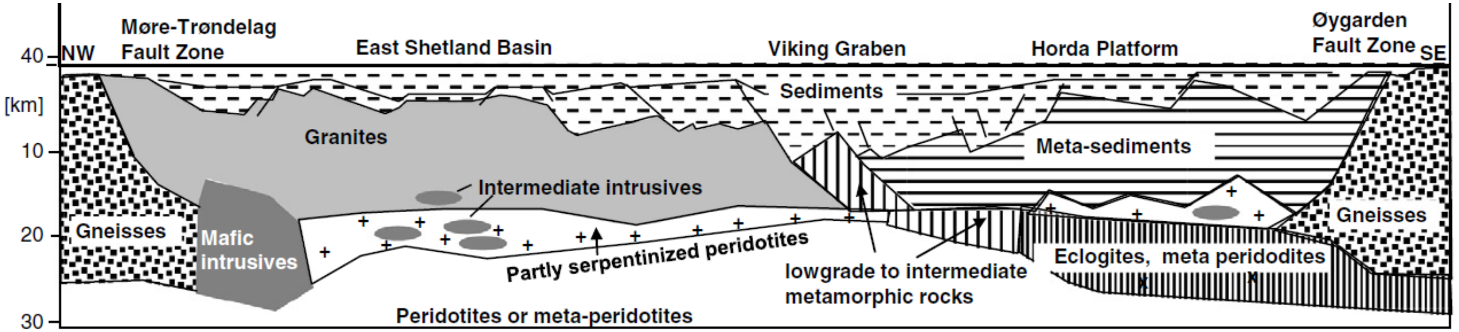

METHODS

NAVIGATION MAP

1. Literature
- Reference Geological Setting
- Area of Interest – State of Art

2. Data Collection
- Seismic Reflection Profile
- Borehole Data
- Potential Field Data
- Literature Data

→
- Deep Layer Velocity
- Deep Layer Density
- Magnetic Susceptibility

3. Data Analysis
- Seismic Interpretation
- Wireline Log Analysis

→
- Velocity Model

→ **Time-to Depth Conversion** → **2D Integrated Gravity Forward Modelling**

→
- Density Model
- Curie Boundary
- Moho Boundary

→ **2D Integrated Gravity Forward Modelling**

4. Results
- Basin Thickness
- High-Susceptibility Sources

5. Conclusions

Borehole Data

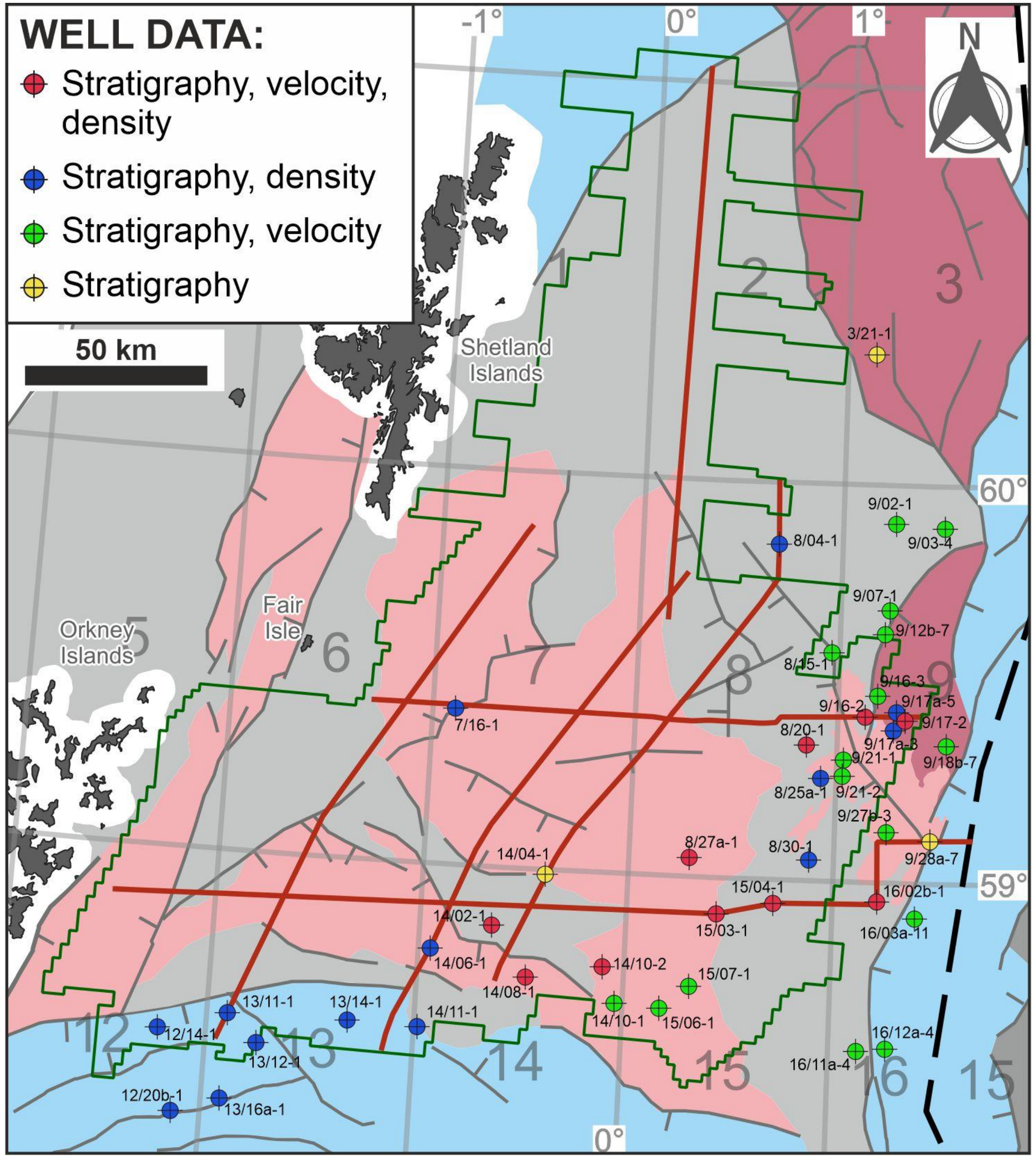

Data from the **43 wells** used in this study were retrieved from the UK National Data Repository (NDR – NSTA, 2022).

The **seismic velocity** data were retrieved from **26 wells** among the total selected wells. These data were used to tie the seismic time-to-depth conversion.

The modelling of the observed gravity anomalies was derived from the **mean density (ρ)** of each chronostratigraphic layer calculated **from wireline bulk density logs** available from **25 wells** within and surrounding the study area.

STRATIGRAPHY - LITHOLOGY → **Geological Constrains**

TIME-DEPTH CHART →
- **Seismic-to-well tie**
- **Velocity Model**

→ **Time-to-Depth Conversion**

BULK DENSITY (ρ) → **Density Model** → **Gravity Model**

SEISMIC INTERPRETATION

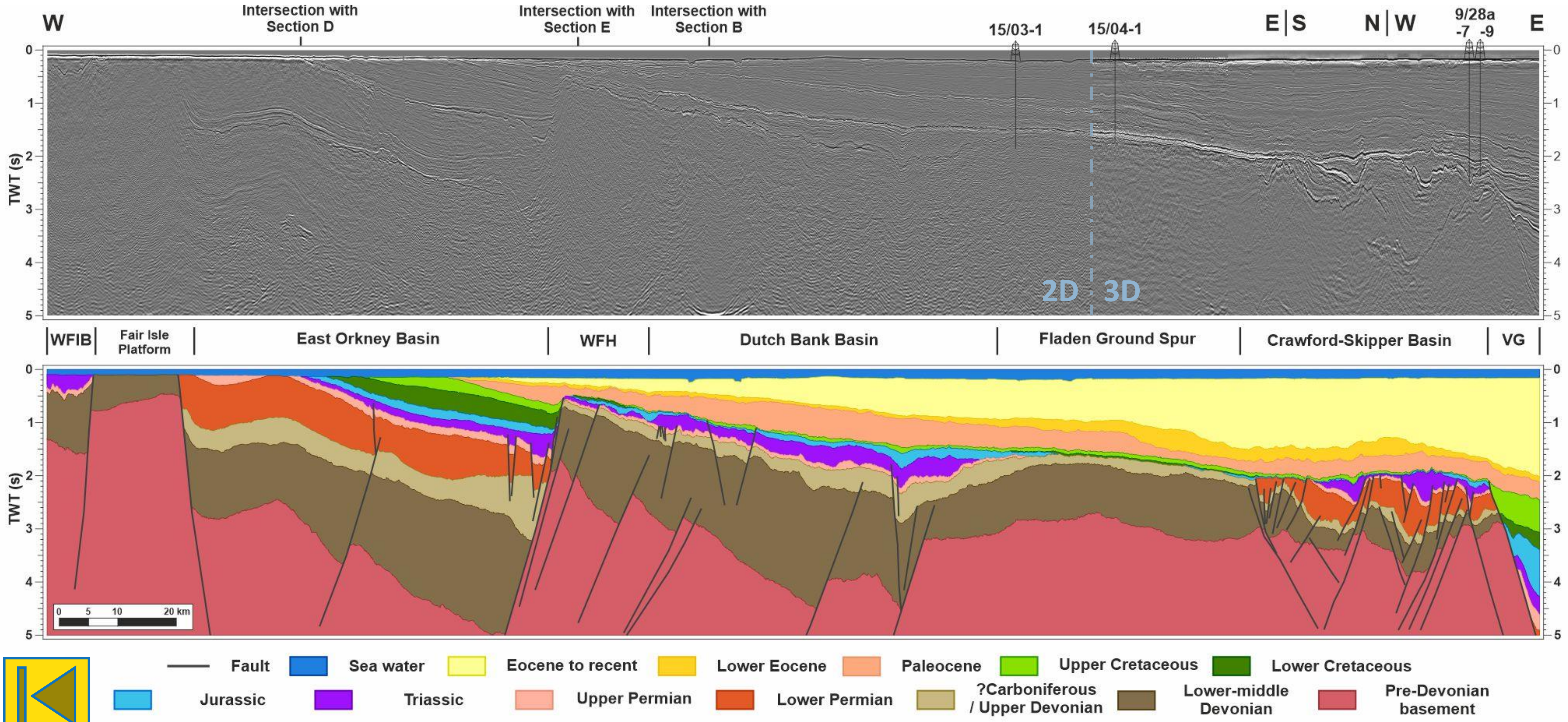

MODELLING PARAMETERS

CHRONOSTRATIGRAPHY	SEISMIC VELOCITY (m s^{-1})	DENSITY (ρ, kg m^{-3})	SUSCEPTIBILITY (k, SI)
Sea Water	1500[1]	1030[2]	—
Eocene to Recent (EtR)	1907 (1461 - 2253)	1997 - 2011 (1610 - 2156)	—
Lower Eocene (LE)		2021 - 2070 (1963 - 2129)	—
Paleocene (P)		2094 (1969 - 2240)	—
Upper Cretaceous (UK)	3725 (2399 - 5177)	2239 - 2563 (2239 - 2647)	—
Lower Cretaceous (LK)	3436 (2931 - 4397)	2232 - 2479 (1626 - 2571)	—
Jurassic (J)	2675 (1458 - 4705)	2072 - 2393 (2072 - 2451)	—
Triassic (T)	3515 (2813 - 4518)	2070 - 2385 (2070 - 2470)	—
Upper Permian (UP)	4526 (3192 - 5357)	2442 - 2587 (2428 - 2832)	—
Lower Permian (LP)	4558 (3859 - 5765)	2300 - 2558 (2292 - 2521)	—
Carboniferous? - Upper Devonian? (CuD)	4067 (3360 - 5460)	2335 - 2670 (2335 - 2670)	—
Lower-middle Devonian (emD)			
Basement (B)	6000[1]	2700[2]	0.001 - 0.05[3]
Lower Crust (LC)	—	2900[2]	0 - 0.05[3]
Mantle (M)	—	3200[2]	—

Simplified stratigraphic column showing the **layers** and relative values of **seismic velocity, density and magnetic susceptibility** adopted for time-to-depth conversion of seismic profiles and gravity and magnetic modelling.

The values **within brackets** indicate **minimum and maximum values** retrieved **from** the available **borehole data**.

Bold values were used for the depth-conversion and modelling.

Reference values from: ([1]) Kearey et al. (2002) and Reynolds (2011); ([2]) Lyngsie and Thybo (2007); and ([3]) Fichler et al. (2011) and Beamish et al. (2016).

POTENTIAL FIELD DATA

TAP MAPS TO VIEW FILTERING

BOUGUER GRAVITY

(red. density of 1800 kg m^{-3})

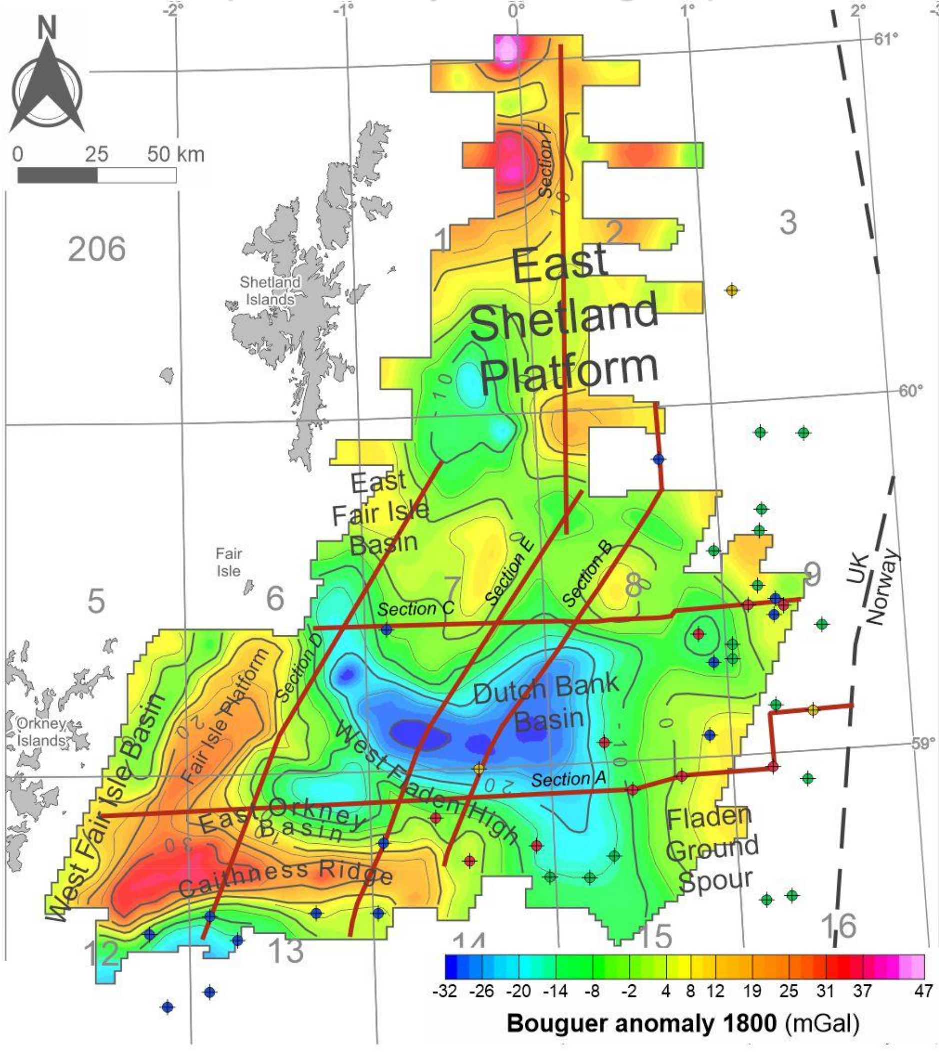

MAGNETIC ANOMALY

(reduced to the pole)

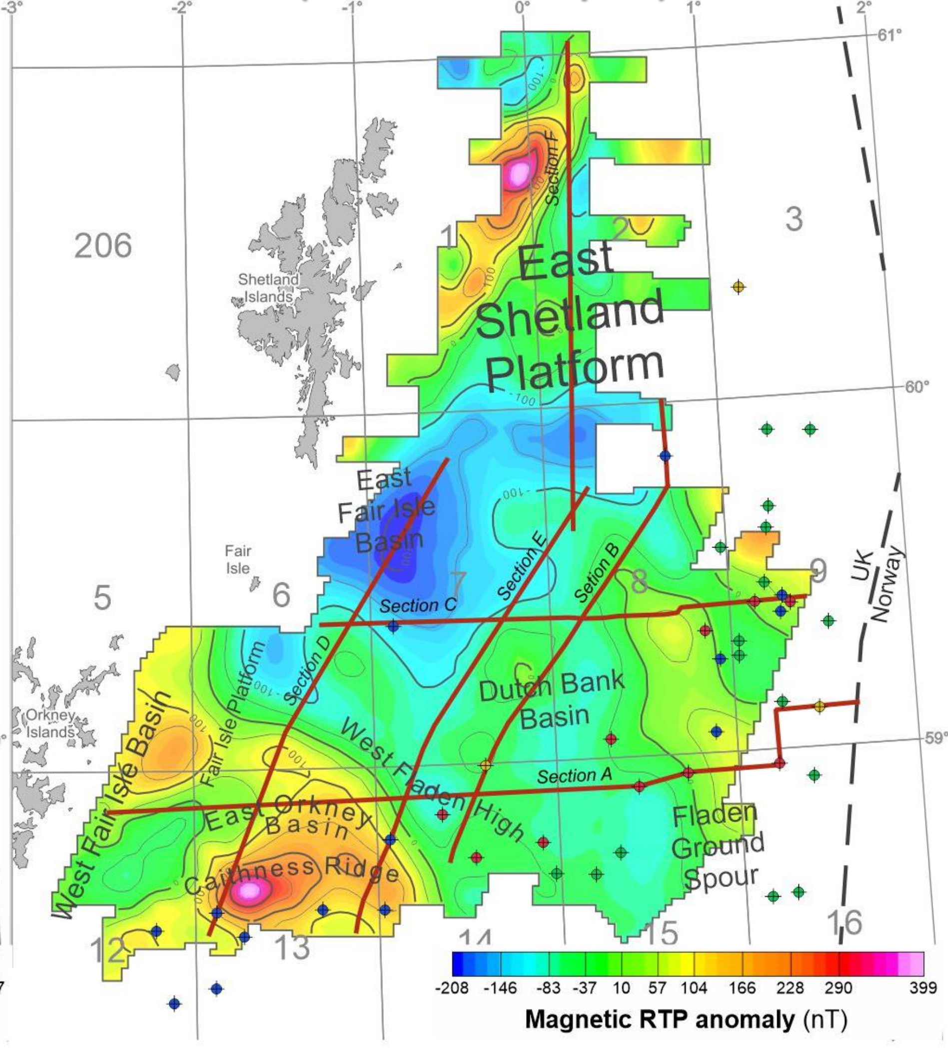

Modelled section — EEZ — WELL DATA: Stratigraphy; Stratigraphy and velocity; Stratigraphy and density; Stratigraphy, velocity and density

(a) **The Bouguer gravity anomaly** dataset was filtered with a 6 km cut-off Gaussian filter, interpolated on a regular **2x2 km grid** and calculated with a **reduction density of 1800 Kg m^{-3}.**

(b) **The magnetic anomaly** data were interpolated on a **2x2 km grid**, **reduced to the pole (RTP)** and filtered using a Gaussian filtering with an 8 km cut-off.

Contour spacing is:

(a) 5 mGal (1 mGal=10^{-5} m s^{-2});

(b) 50 nT.

BOUGUER TOTAL AND FILTERED ANOMALY

TOTAL

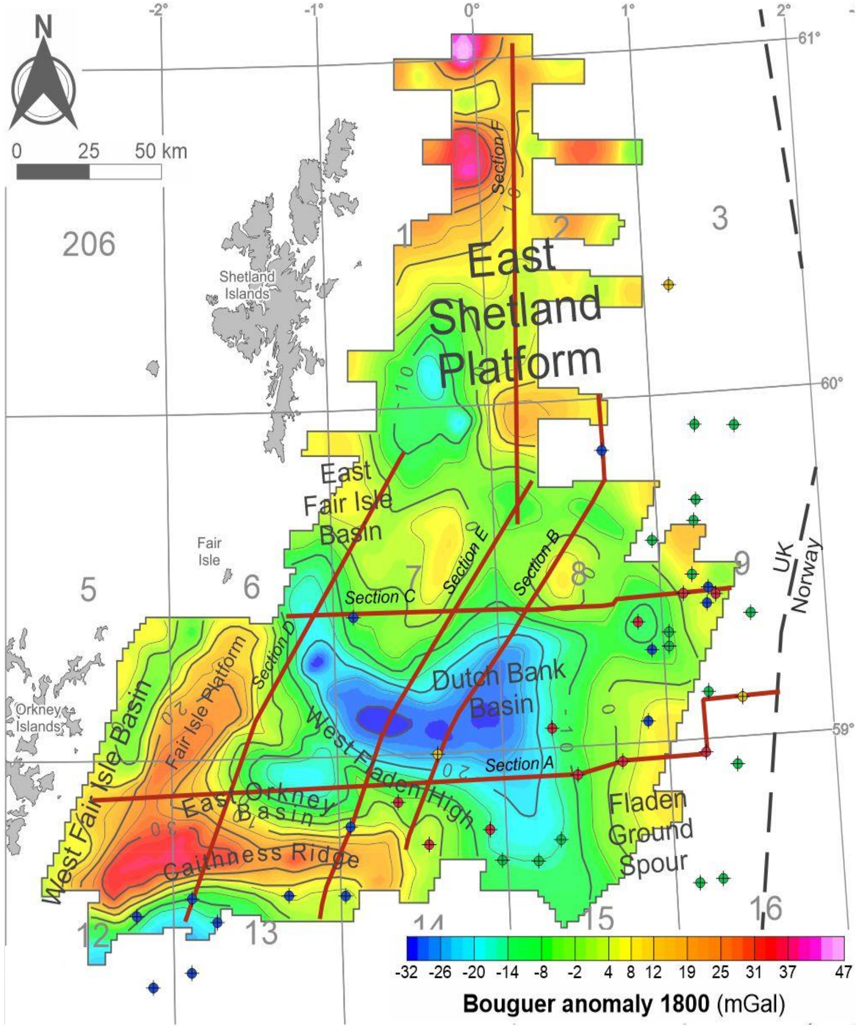

High-Pass 50 km

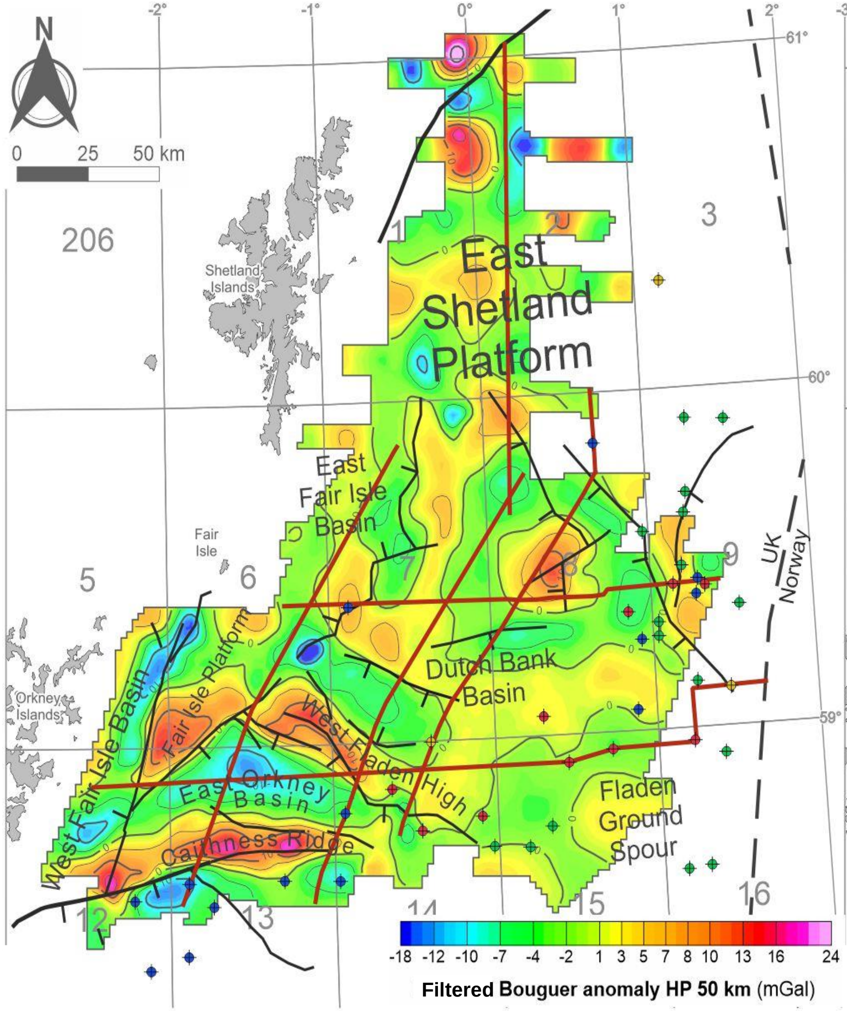

Low-Pass 50 km

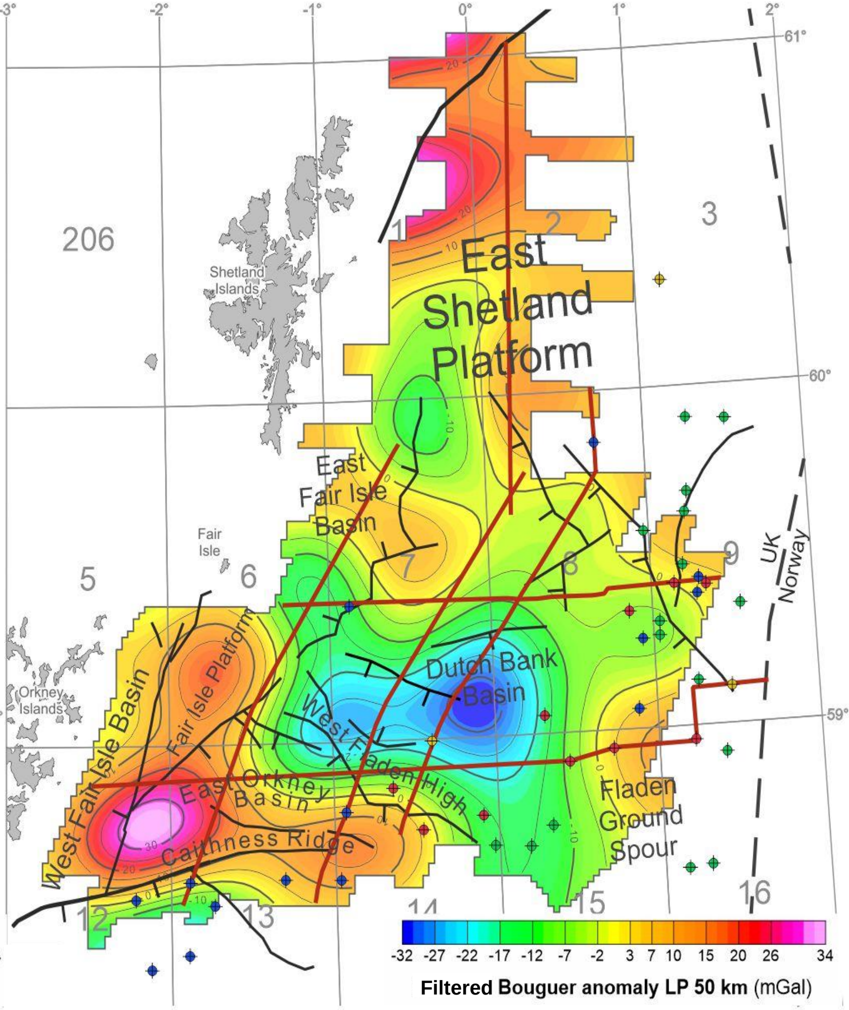

MAGNETIC TOTAL AND FILTERED ANOMALY

TOTAL

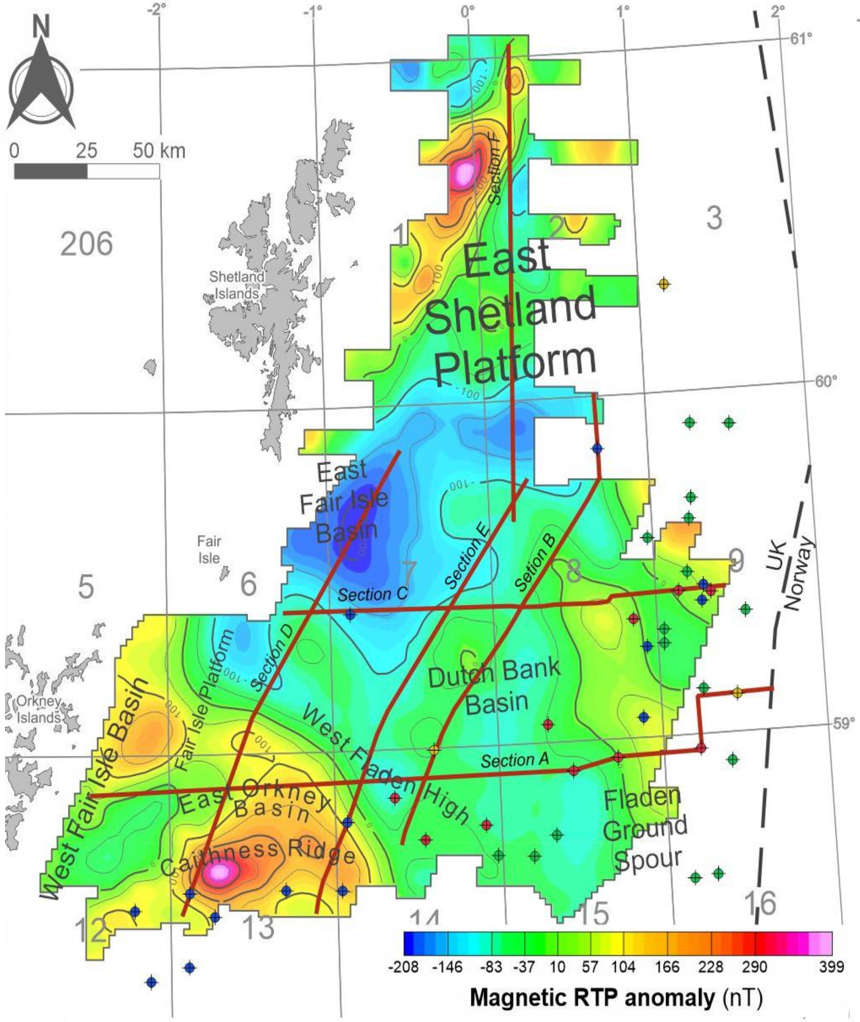

High-Pass 50 km

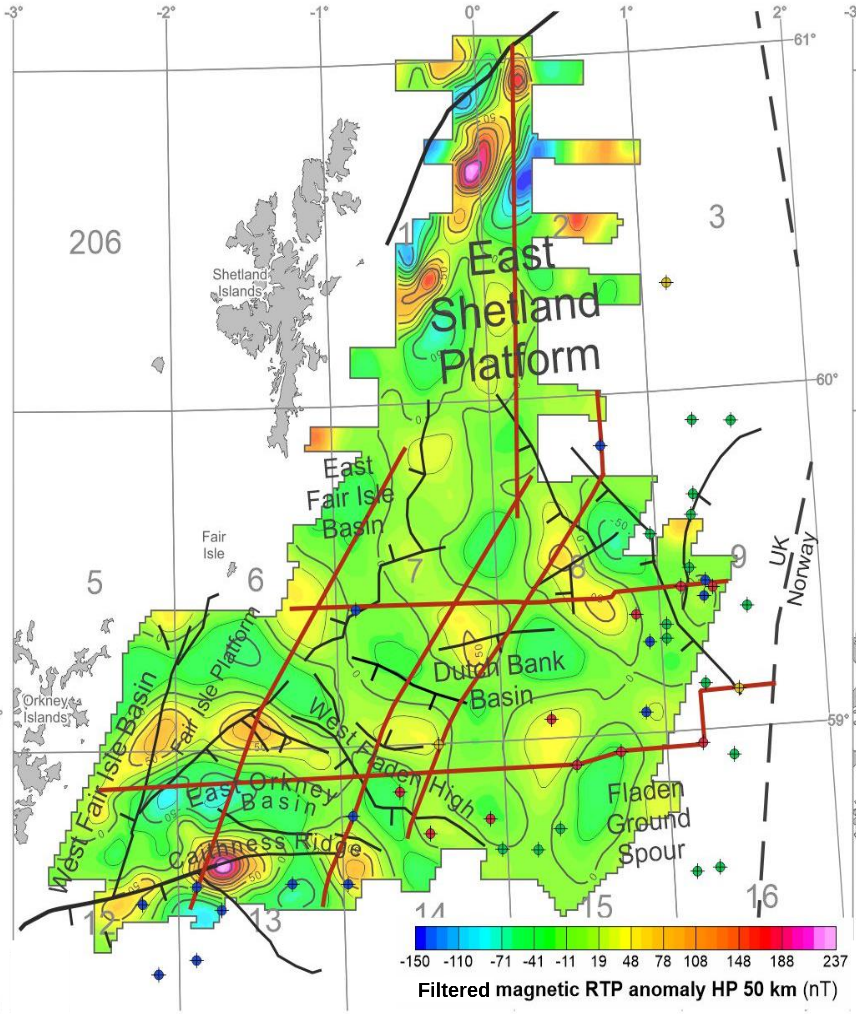

Low-Pass 50 km

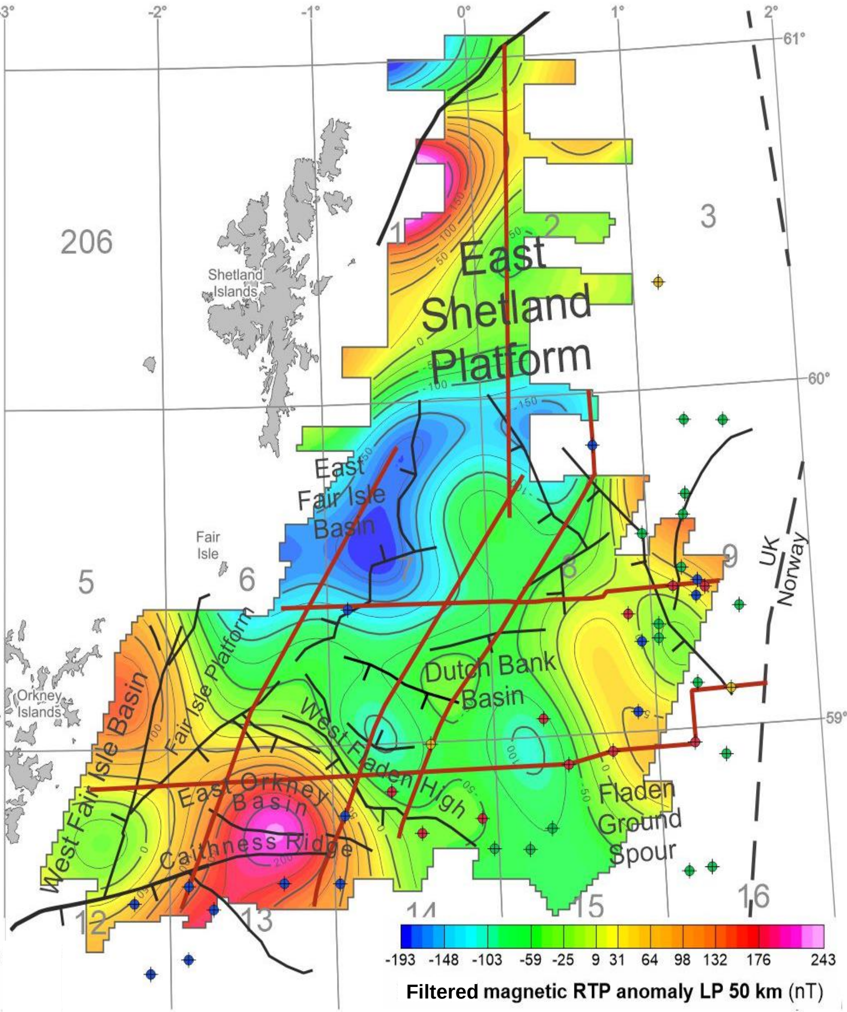

MESOZOIC TIME THICKNESS VS. BOUGUER GRAVITY

Mesozoic Time (TWT) Thickness map compared with contours of the Bouguer Gravity

Color scale represents the time thickness grid of the Mesozoic sequence.

Black lines represent the contour of Bouguer total anomaly (contour interval 5 mGal).

Thin red lines are traces of the interpreted 2D seismic lines (NSTA, 2022) used to calculate the time thickness maps; thick red lines show the sections modelled in this work.

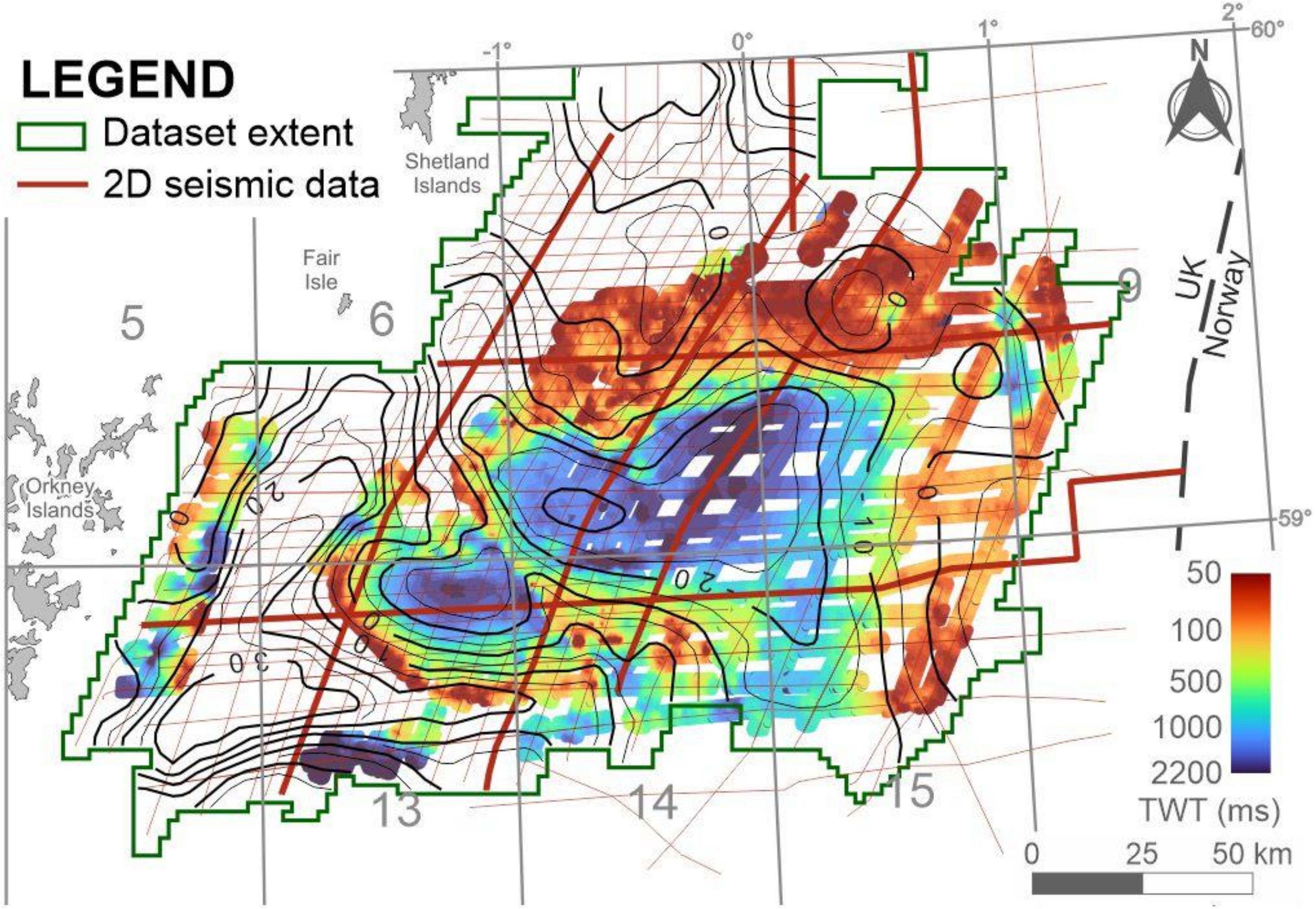

SECTION A - MODEL

DEPTH-CONVERTED MODEL

ANOMALY BEST FITTING

2D GRAVITY AND MAGNETIC MODELLING

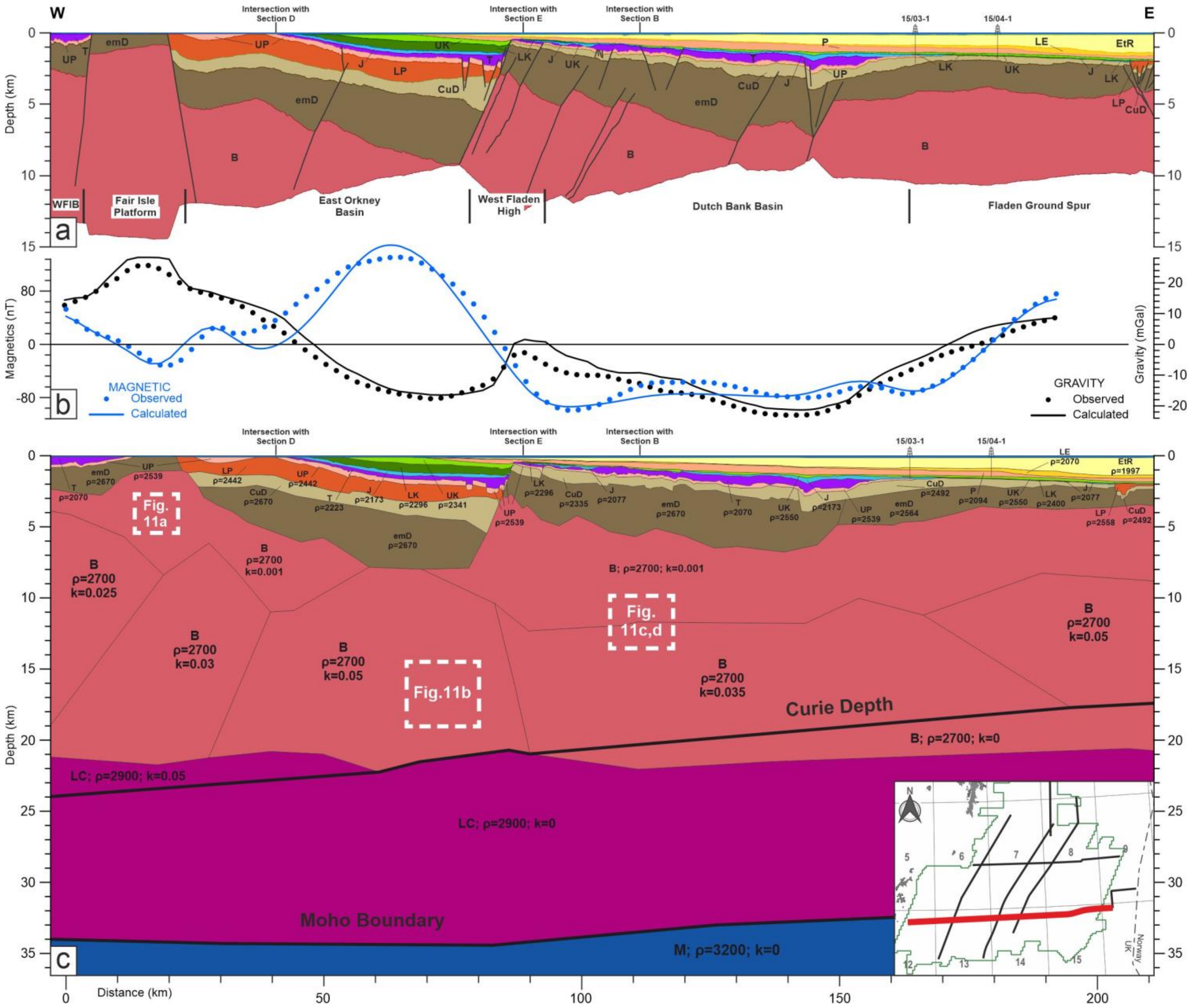

Modelled density (ρ) and magnetic susceptibility (k) values are given for each block in the lower panel. White dashed boxes locate seismic samples.

Section B - Model

Depth-Converted Model

Anomaly Best Fitting

2D Gravity and Magnetic Modelling

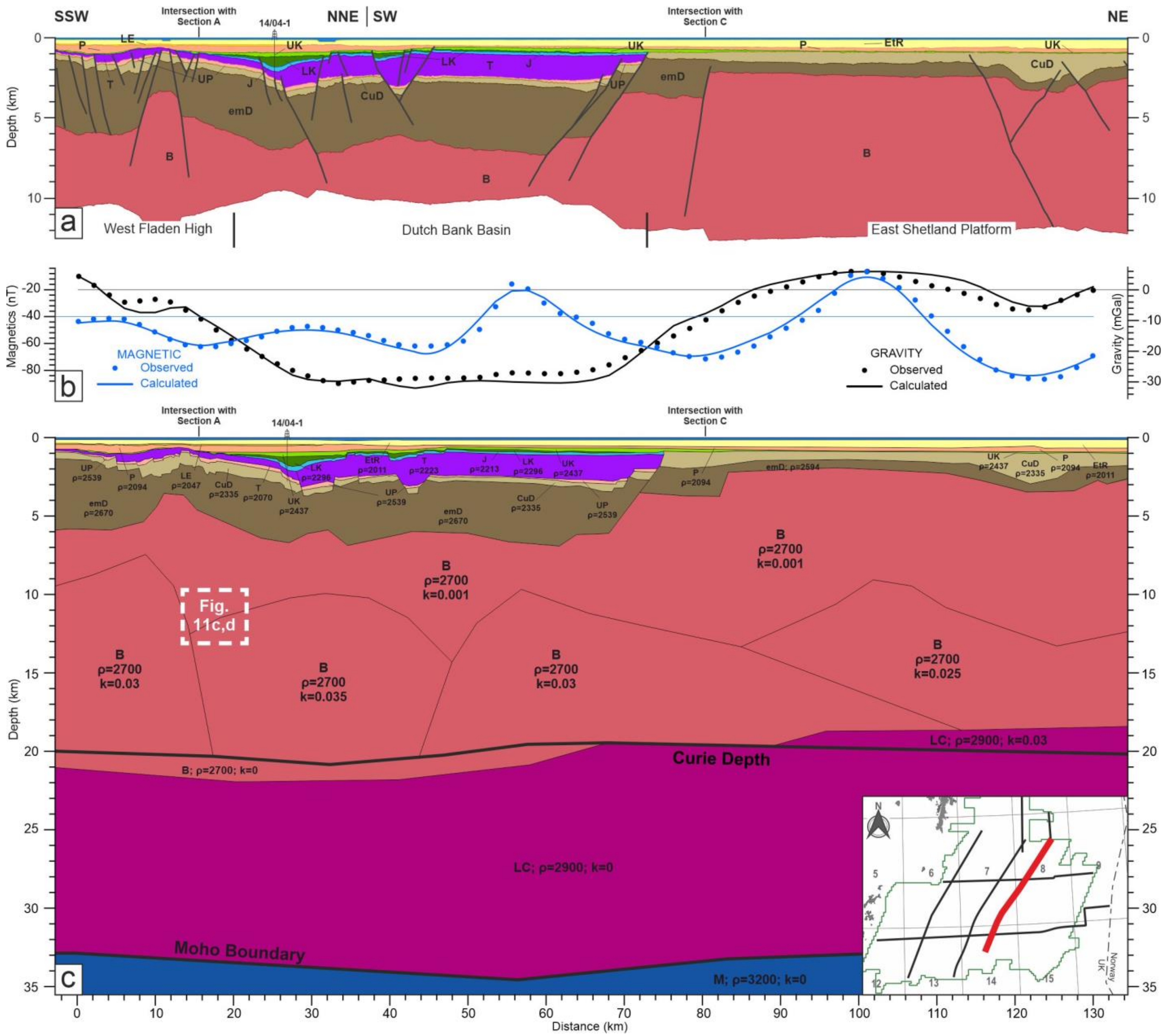

Modelled density (ρ) and magnetic susceptibility (k) values are given for each block in the lower panel. White dashed boxes locate seismic samples.

Section C - Model

Depth-Converted Model

Anomaly Best Fitting

2D Gravity and Magnetic Modelling

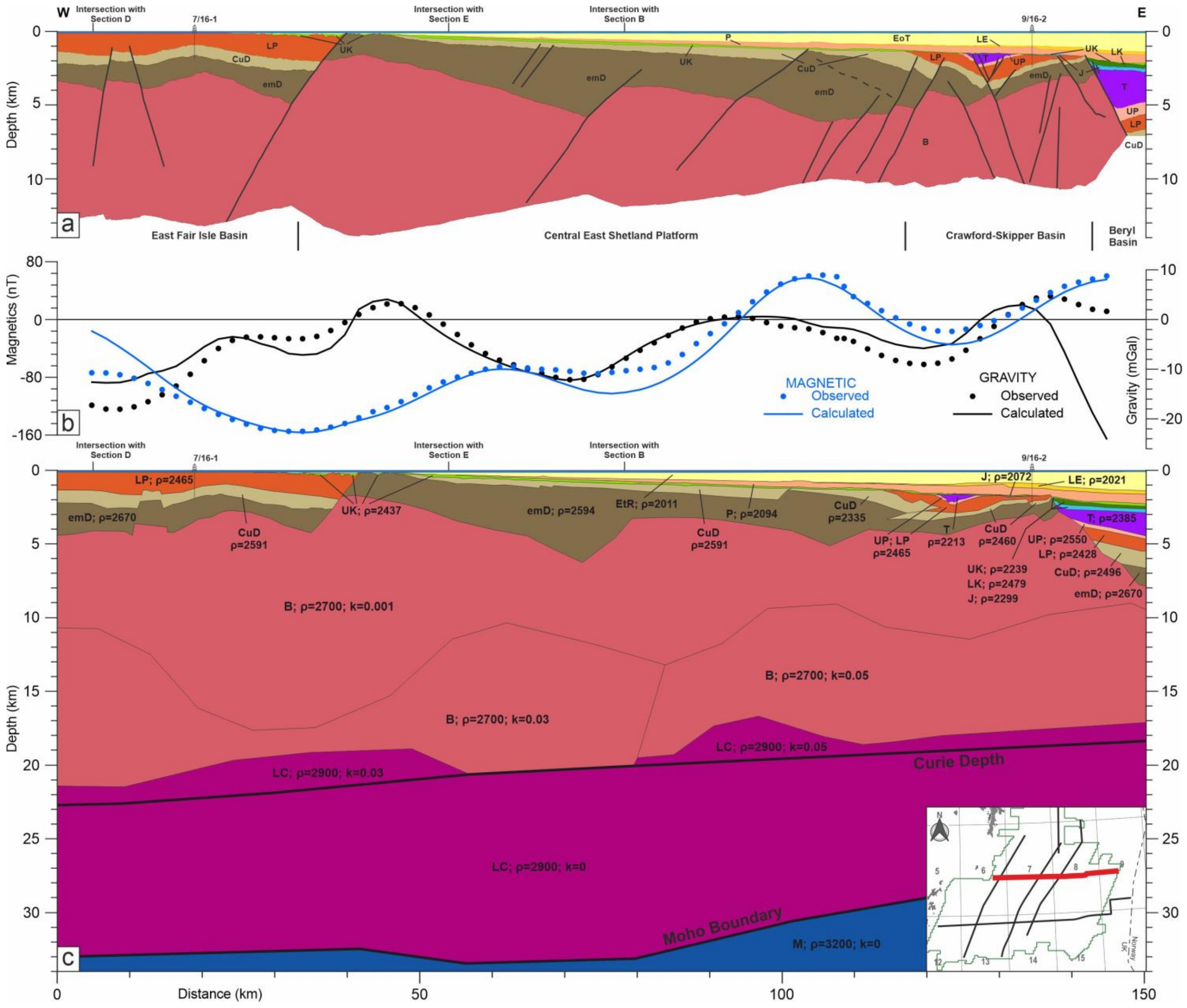

Modelled density (ρ) and magnetic susceptibility (k) values are given for each block in the lower panel. White dashed boxes locate seismic samples.

SECTION D - MODEL

DEPTH-CONVERTED MODEL

ANOMALY BEST FITTING

2D GRAVITY AND MAGNETIC MODELLING

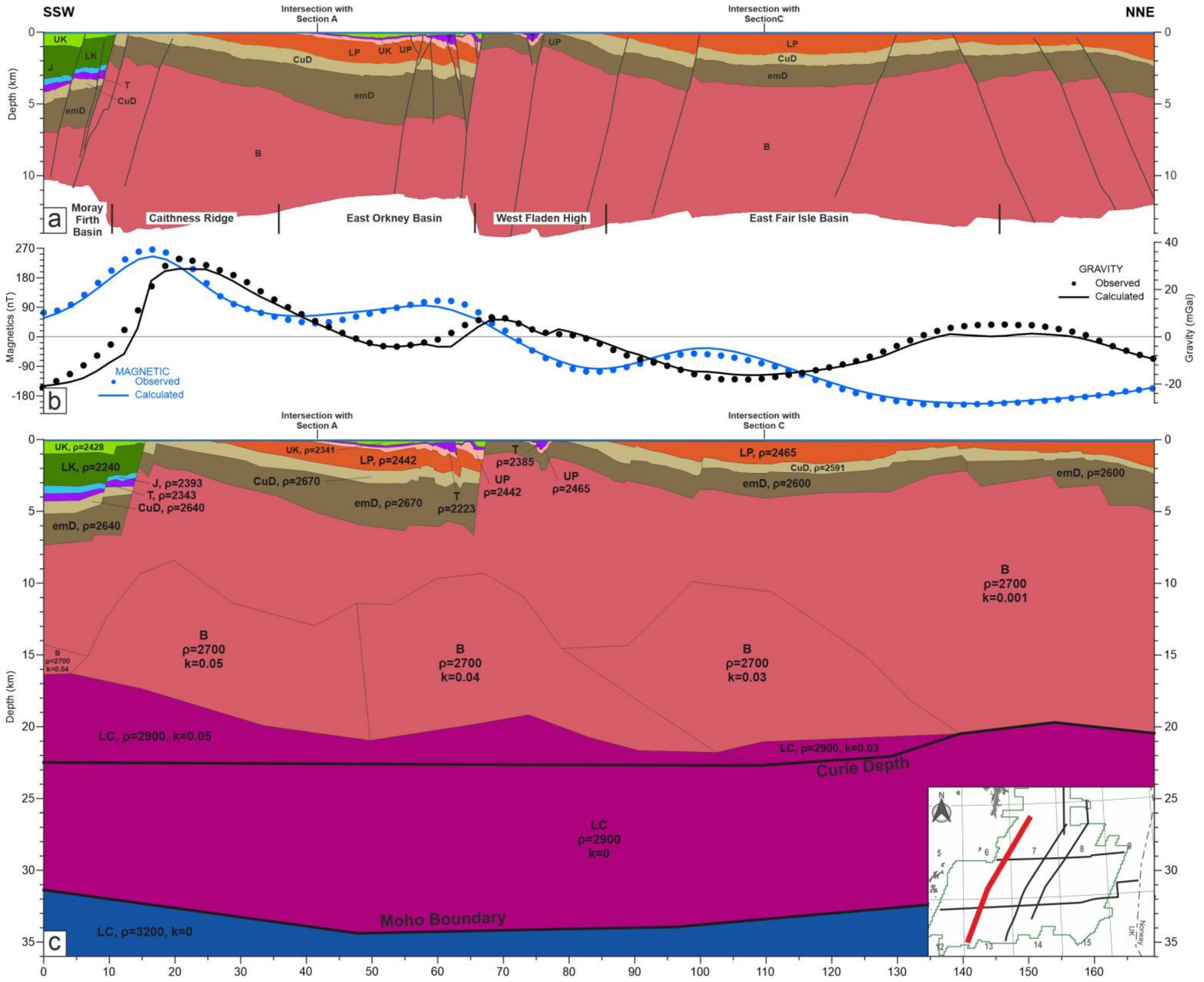

Modelled density (ρ) and magnetic susceptibility (k) values are given for each block in the lower panel. White dashed boxes locate seismic samples.

SECTION E - MODEL

DEPTH-CONVERTED MODEL

ANOMALY BEST FITTING

2D GRAVITY AND MAGNETIC MODELLING

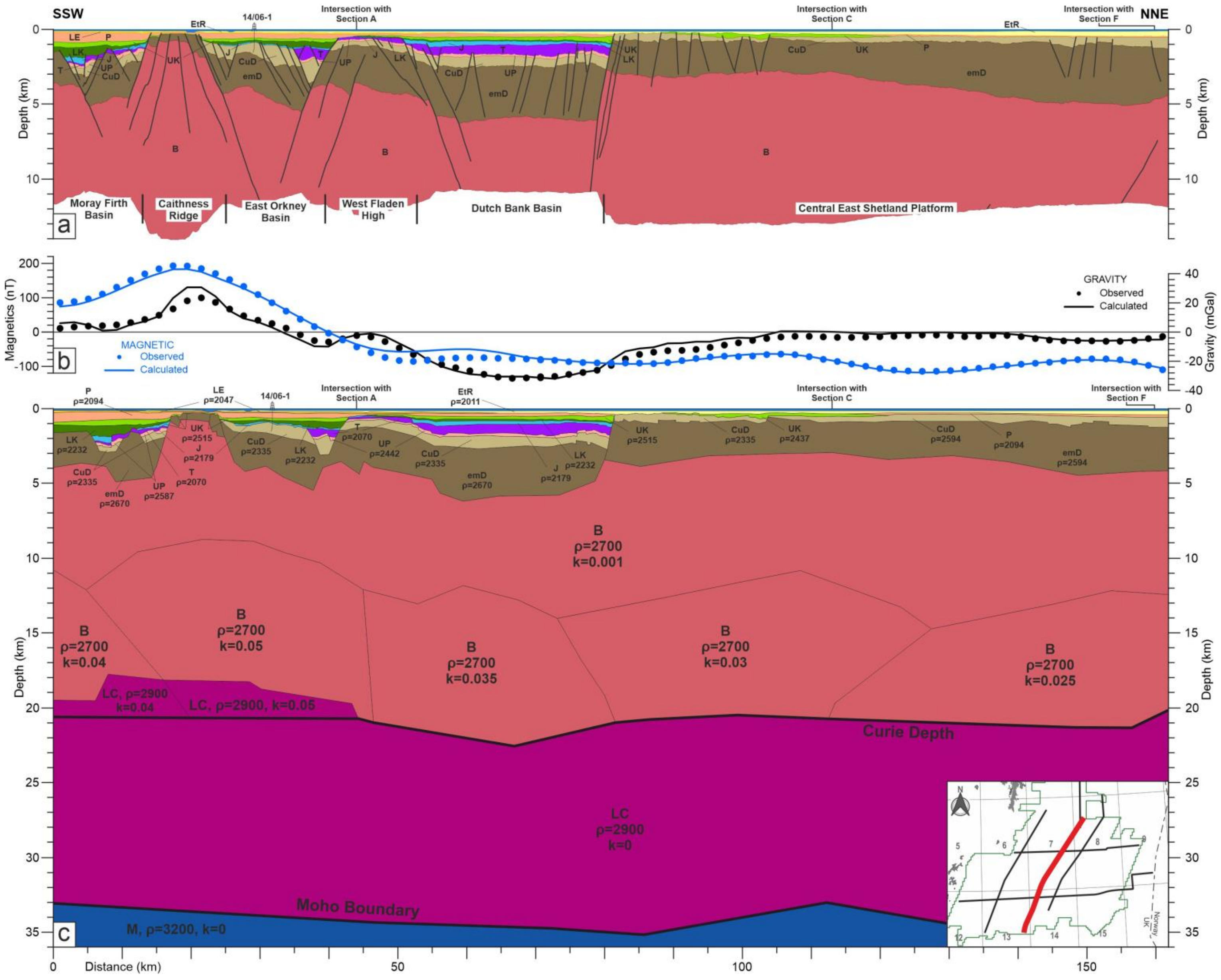

Modelled density (ρ) and magnetic susceptibility (k) values are given for each block in the lower panel. White dashed boxes locate seismic samples.

SECTION F - MODEL

DEPTH-CONVERTED MODEL

ANOMALY BEST FITTING

2D GRAVITY AND MAGNETIC MODELLING

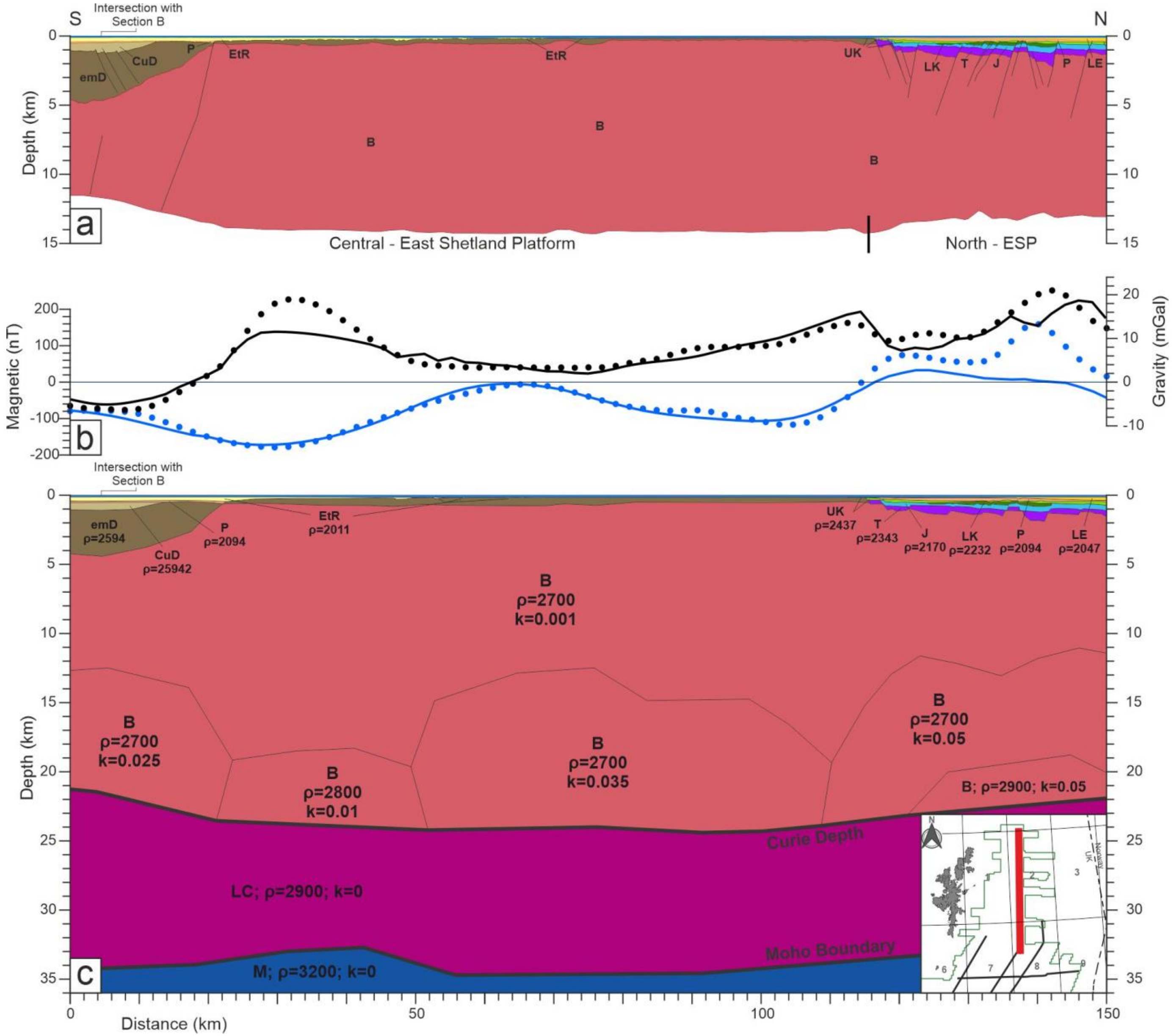

Modelled density (ρ) and magnetic susceptibility (k) values are given for each block in the lower panel. White dashed boxes locate seismic samples.

Basin Thickness

Upper Cretaceous

Lower Cretaceous

Jurassic + Triassic

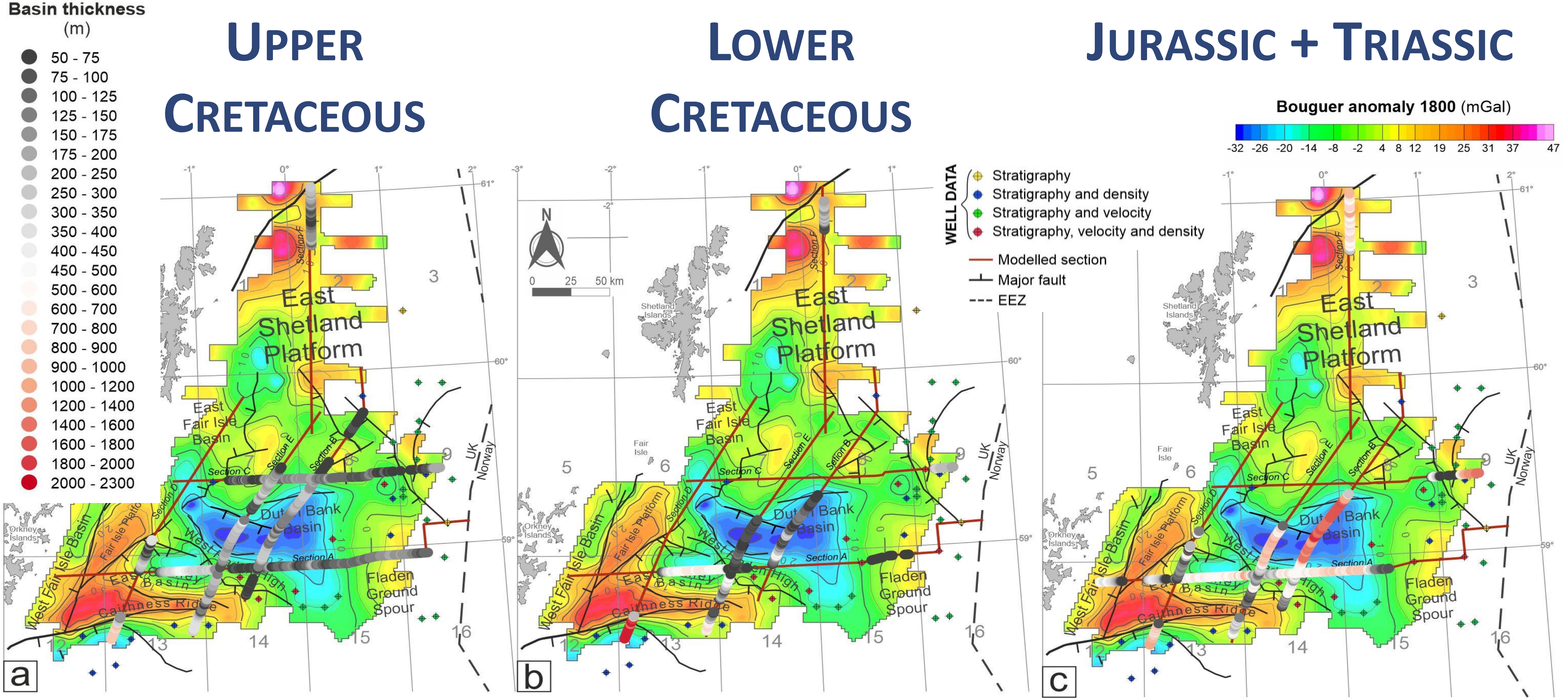

Section A - Section B - Section C - Section D - Section E - Section F

Seismic Amplitude Variations

Portions of seismic reflection profiles showing the different reflectivity of basement and crust in the study area.

(a) **Low-reflectivity** zones (high-frequency, low-amplitude and discontinuous reflections) match with **low magnetic blocks**.

(b, c, d) **High-reflectivity** zones (low-frequency, high-amplitude and laterally continuous reflections) generally correspond to **high-susceptibility blocks**.

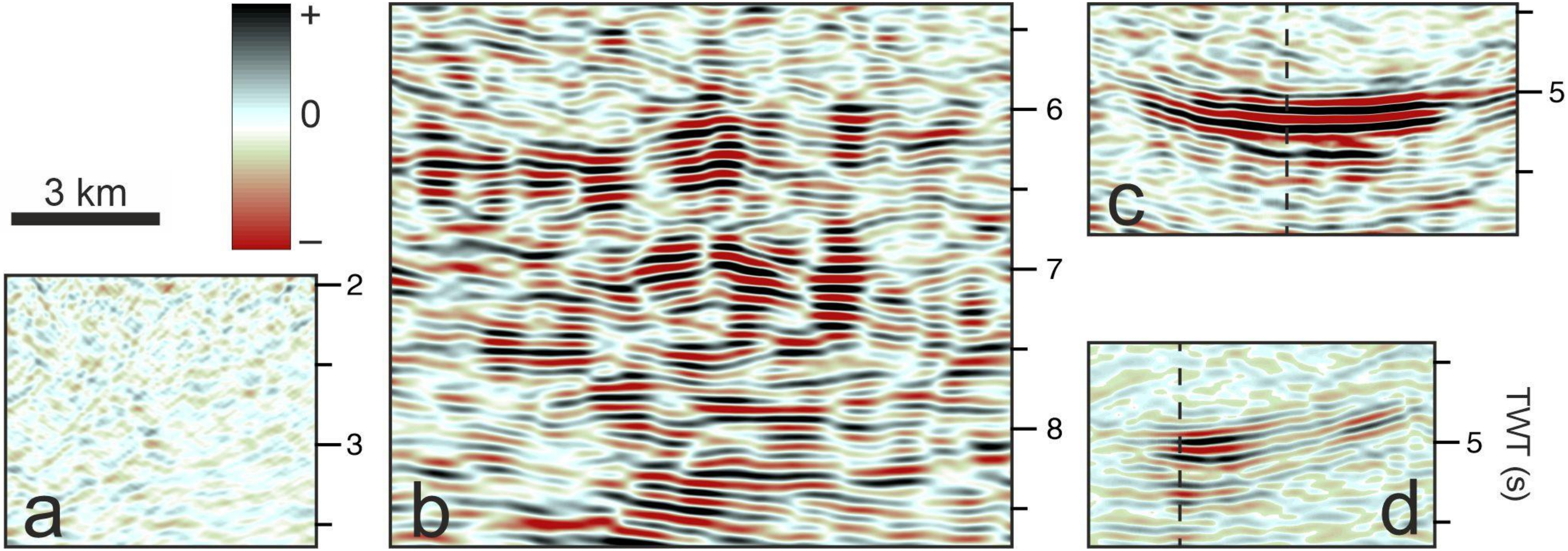

Section A
Section B

HIGH SUSCEPTIBILITY SOURCES

Filtered magnetic dataset (50 km low-pass)

The thick dashed lines enclose **areas** where the **same magnetic susceptibility** (*k*) was used to model the basement. These all refer to **15 km depth.**

- Black lines locate areas with **high-susceptibilities** (**0.025-0.05** SI units)
- Blue lines encloses the area with **low-susceptibility** (**0.001** SI units) basement.

The thick dashed ***red line*** encompasses the area proposed as ***serpentinized crust by Fichler et al. (2011).***

High-*k* rock samples refer to onshore gabbroid or serpentinized rocks (BGS, 2022).

Diamonds locate well cores classification referring to the basement (Bassett 2003).

Abbreviations: Grn, granite; Qzt, quartzite; Metased, meta sediment; Amp, amphibolite; Gab, gabbro; Sch, schist; Gns, gneiss; Migm, migmatite.

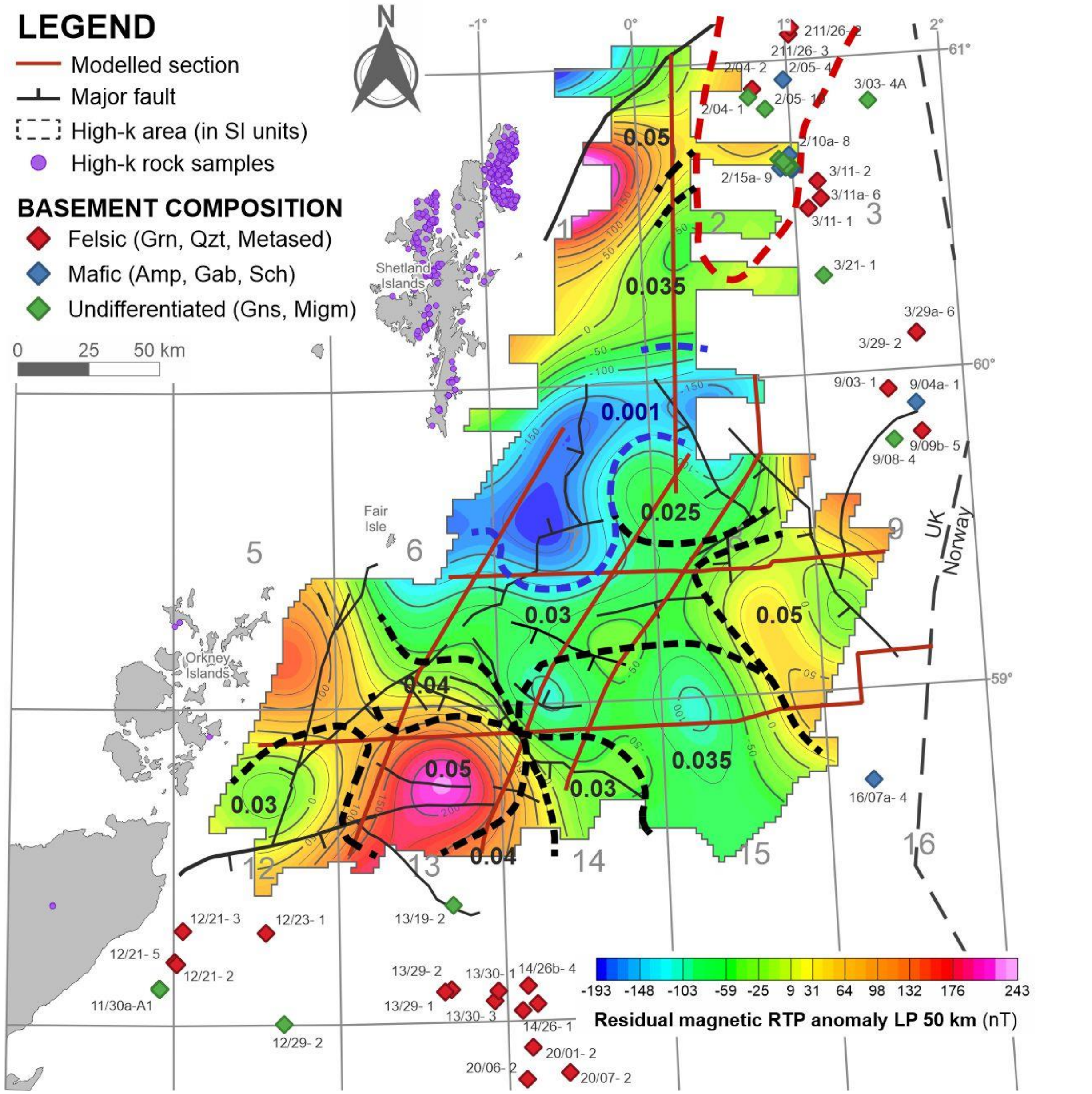

CONCLUSIONS AND FUTURE STEPS

EGU General Assembly #EGU23 23 - 28 April 2023

1. BOUGUER LOWS

Mesozoic sedimentary sequences

- Dutch Bank Basin – Triassic and thin Jurassic infilling;
- East Orkney Basin – Tectonic subsidence during the Lower Cretaceous.

2. BOUGUER HIGHS

Areas **with reduced sedimentary cover** and shallowing basement.

Mainly consisting of Devonian sediments (e.g., the Caithness Ridge).

3. MAGNETIC ANOMALY

Low-susceptibility blocks within the **upper basement**

compatibility with acoustically-opaque metamorphosed sediments and granitoid/alkaline igneous rocks.

High-susceptibility blocks within the **lower basement**

compatibility with mafic bodies and serpentinized crust. These show in reflection seismic as a widespread high-amplitude and low-frequency layers. These are the main contributors to the observed magnetic anomaly.

4. GEODYNAMIC

The high-susceptibility and high-reflective volumes can be related to **structural paleo-domains connected to the Caledonian orogeny** and the **pre-Caledonian Iapetus Ocean**.

Future Steps

Some of these **basins are close to the UK shorelines** and are **crosscut by existing pipelines.**

We will address their **potential for geological carbon storage** (CCS), considering also their closeness to recent CCS project area (e.g., Acorn, Sleipner and Northern Lights projects).

ABSTRACT

February 21, 2023
Paper submitted to Elsevier – Tectonophysics

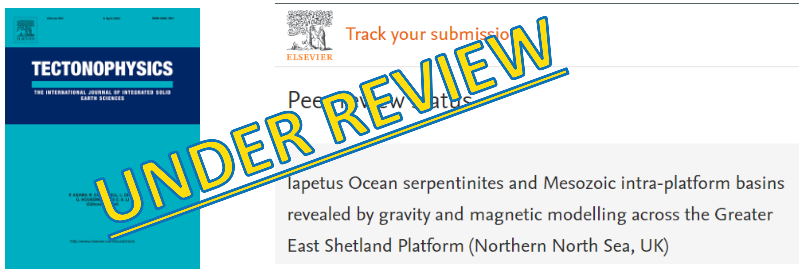

THANK YOU FOR YOUR INTEREST

SEISMIC REFLECTION DATA

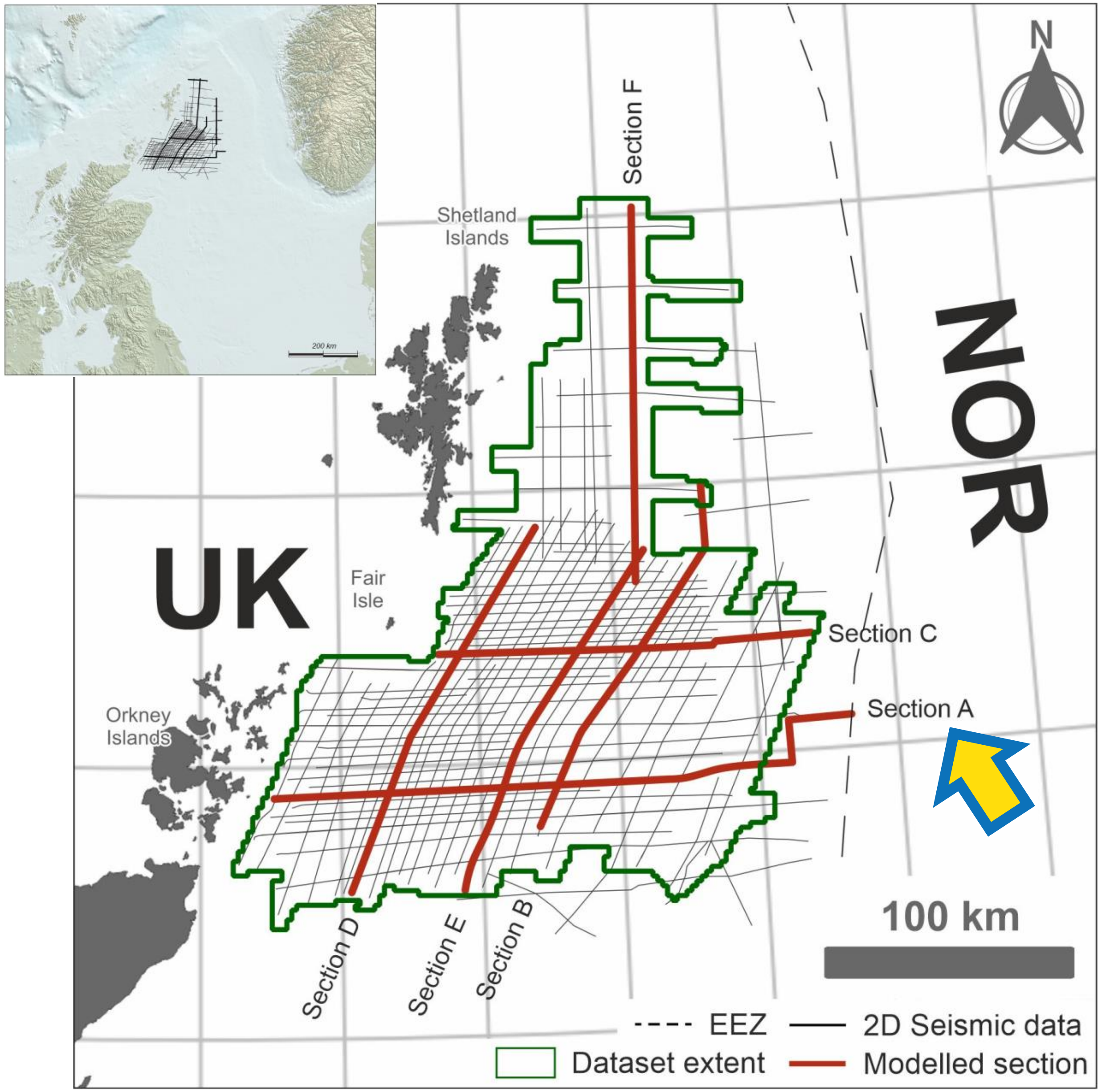

NAME	LINE LENGHT (km)	
	Total	**Modelled**
Section A	253	195
Section B	161	133
Section C	150	all
Section D	164	all
Section E	155	all
Section F	154	all
TOTAL	1037	709

The **six lines** (**total line-length** of about **1046 km**) investigated in this work have been selected from a **2D regional broadband seismic dataset** (Survey PP162DGOGA, total line-length of about 15,000 km) covering the Greater East Shetland Platform (GESP).

This 2D survey was **acquired and processed by PGS** (2017) in 2016-2017 for the UK Oil & Gas Authority (OGA, now NSTA) and subsequently freely distributed to industry and academia via the NDR online platform.

These lines extend until **5 sec TWT** depth highlighting a clear **distinction between the shallow and deep reflectors**.

The **Top Zechstein** reflector (Base Triassic-Top Upper Permian) marks a distinctive **change in the seismic facies** with a high amplitude, laterally continuous bright trough. Above this, medium to high-amplitude laterally continuous reflectors can be observed. Directly beneath the Top Zechstein reflector, there are opaque low amplitude seismic facies until low-frequency high-amplitude zones are reached at depth.

Seismic Velocity Model

The simplified **interval velocity model** has been **used** to the **time-to-depth conversion**. This model provides an average value for each chronostratigraphic interval (Glover, 2000).

The conversion function was guided by the following relationship (Etris et al., 2002):

$$Z = V_0 \frac{e^{kt} - 1}{k}$$

where Z is the thickness of the layers in meters, V_0 is the velocity at the top of the layer in m s^{-1}, κ corresponds to the variation frequency of the velocity with the increase in depth and t indicates the one-way time (t = TWT/2) for the layer thickness in seconds.

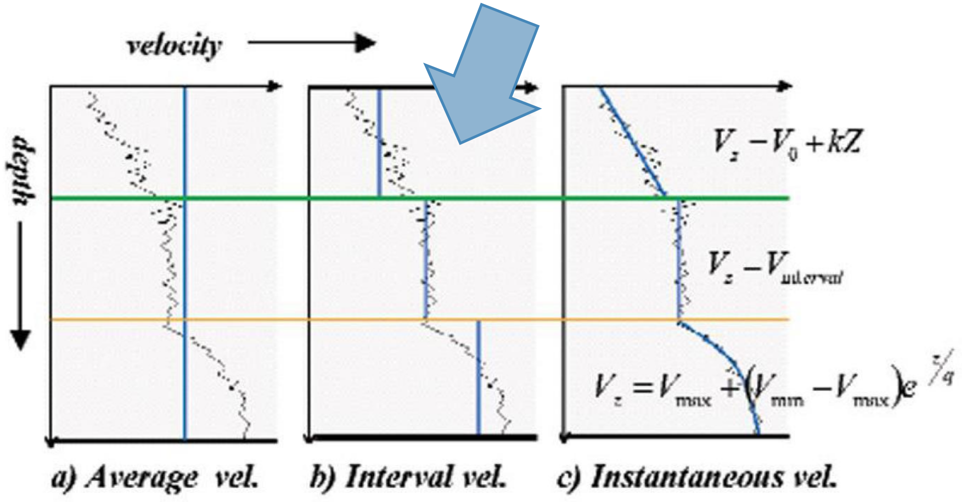

Modified from Etris et al. (2022)

CHRONOSTRATIGRAPHY	SEISMIC VELOCITY (m s^{-1})
Sea Water	1500[1]
Eocene to Recent (EtR)	1907 (1461 - 2253)
Lower Eocene (LE)	
Paleocene (P)	
Upper Cretaceous (UK)	3725 (2399 - 5177)
Lower Cretaceous (LK)	3436 (2931 - 4397)
Jurassic (J)	2675 (1458 - 4705)
Triassic (T)	3515 (2813 - 4518)
Upper Permian (UP)	4526 (3192 - 5357)
Lower Permian (LP)	4558 (3859 - 5765)
Carboniferous? - Upper Devonian? (CuD)	4067 (3360 - 5460)
Lower-middle Devonian (emD)	
Basement (B)	6000[1]
Lower Crust (LC)	—
Mantle (M)	—

Simplified stratigraphic column showing the layers and the relative values of seismic velocity. The values within brackets indicate minimum and maximum values retrieved from the available borehole data. Reference values from: ([1]) Kearey et al. (2002) and Reynolds (2011).

Due to the extreme lateral variation of the seismic units and the resulting horizontal changes in seismic velocity with depth, a constant interval velocity model has been adopted to simplify the time-to-depth conversion.

In this case, the κ parameter equals to zero and the previous relationship is simplified as follow:

$$Z = V_0\, t$$

MOHO DEPTH

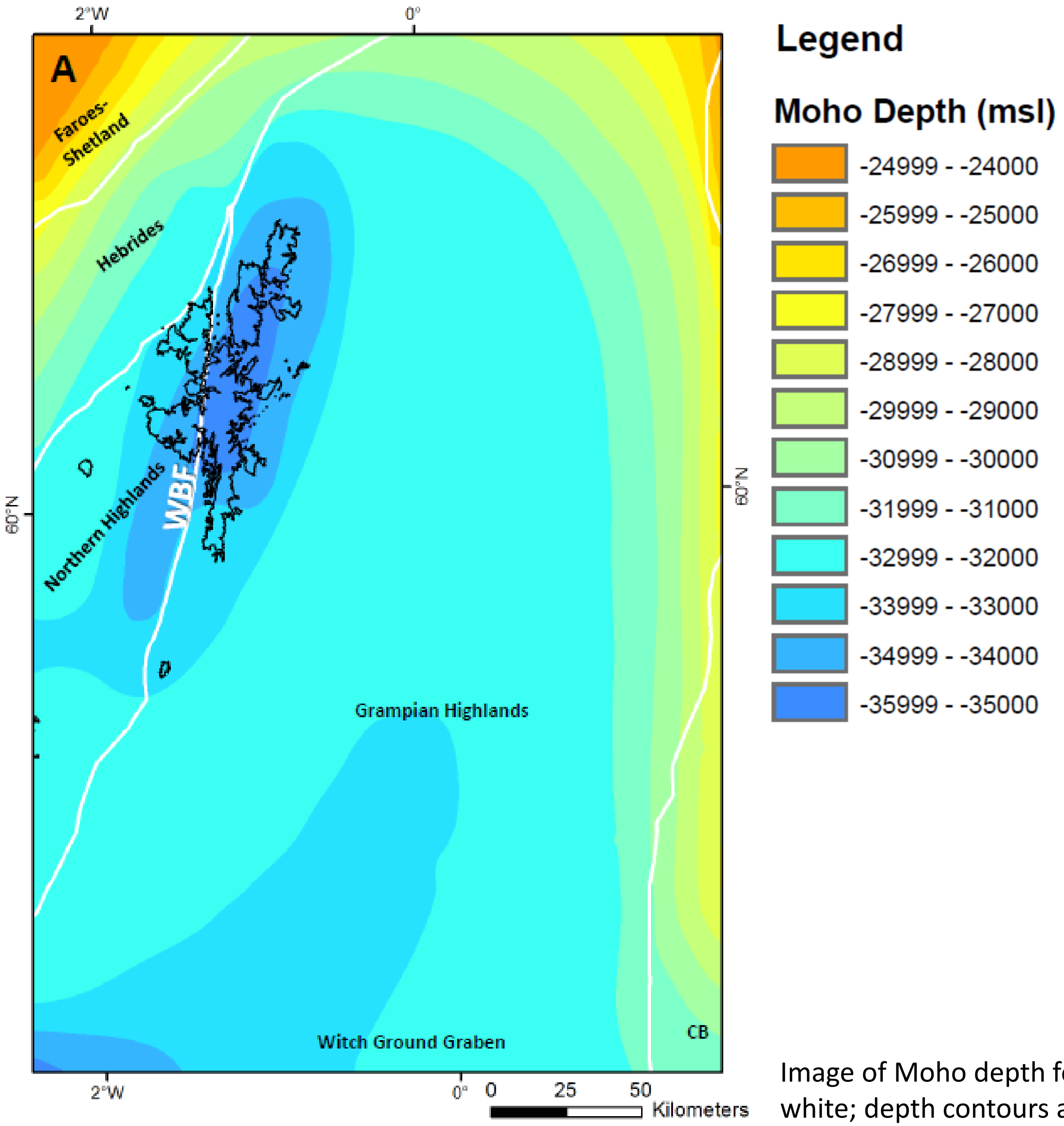

The **Moho** depth (**28-35 km**) was derived from the available literature in the study area and surroundings (Frogtech Geoscience, 2017 and references therein).

Along the modelled 2D profiles, the depth of the Moho discontinuity ranges from about **28 km** eastwards, close to the **Viking Graben,** to about **35 km** westwards, **beneath the Shetland Islands** and the **Moray Firth Basin** (Fichler and Hospers, 1990; Frogtech Geoscience, 2017).

In the **central part** of the study area, the Moho depth is estimated to range between **32 and 34 km**.

Image of Moho depth for the East Shetland Platform, shown with basement terrane boundaries in white; depth contours at 1000 m intervals for Moho depth. (Frogtech Geoscence, 2017)

EGU General Assembly #EGU23 23 - 28 April 2023

CURIE DEPTH

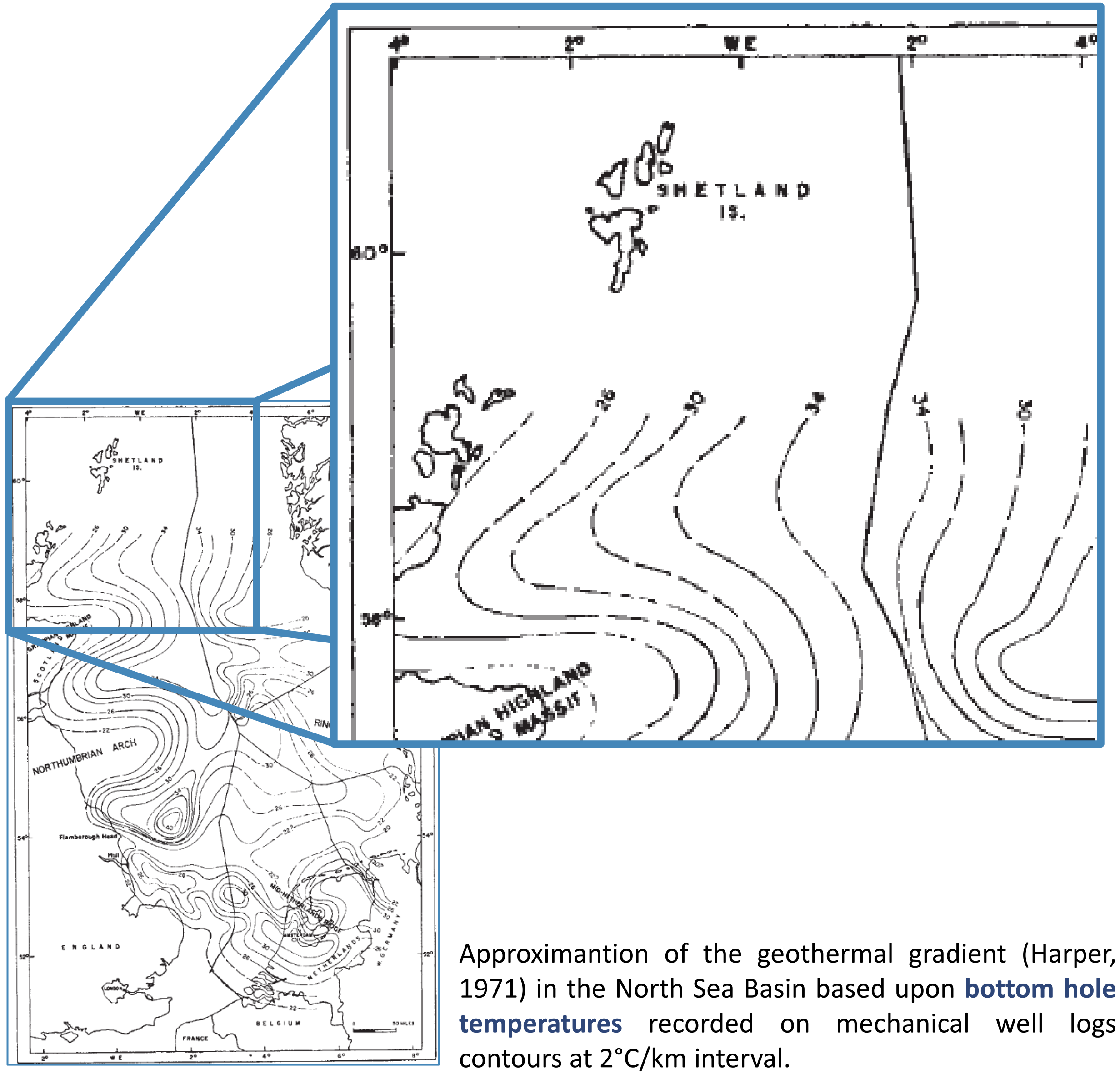

Approximantion of the geothermal gradient (Harper, 1971) in the North Sea Basin based upon **bottom hole temperatures** recorded on mechanical well logs contours at 2°C/km interval.

The **crustal thermal gradient (G_g)** in the area ranges between **26 and 34 °C/km^{-1}** (Harper, 1971).

We assumed a **Curie temperature (C_t) of 600 °C.**

We estimate the **Curie depth (C_d)** to range between **17 and 23 km** with a westward-deepening trend across the entire study area.

Magnetic field parameters:

	VALUE
Survey Year	2016
Latitude	59.31977
Longitude	-0.66587
Inclination	72.121
Declination	-1.907
Magnitude (nT)	50738.2

REFERENCES

Bassett, M.G., 2003. Sub-Devonian geology. In: Evans, D., Graham, C., Armour, A. & Bathurst, P. (Eds), The Millennium Atlas: Petroleum Geology of the Central and Northern North Sea. Geological Society, London, 61–63.

Beamish, D., Kimbell, G., Pharoah, T.C., 2016. The deep crustal magnetic structure of Britain. Proceedings of the Geologists' Association, vol. 127 (3-4), 647–663. http://dx.doi.org/10.1016/j.pgeola.2016.10.007

BGS, 2022. https://mapapps2.bgs.ac.uk/geoindex/home.html (Last visited on October 19, 2022)

Bliss, K., Weston, J., Croft, M., 2016. Processing Report 2d Marine Gravity and Magnetic Data OA16ESP, East Shetland Platform Offshore, UK. Bridgeporth Prj n16_030, Bridgeporth Ltd.

Etris, E.L., Crabtree, N.J., Dewar, J., 2002. True Depth-conversion: More Than a Pretty Picture. Scott Pickford, A Core Laboratories Company, vol. 26 (9).

Fichler, C., Odinsen, T., Rueslåtten, H., Olesen, O., Vindstad, J.E., Wienecke, S., 2011. Crustal inhomogeneities in the Northern North Sea from potential field modelling: Inherited structure and serpentinites?, Tectonophysics, vol. 510, 172–185. https://doi.org/10.1016/j.tecto.2011.06.026

Frogtech Geoscience, 2017. 21 CXRM East Shetland Platform Project Phase 1 - SEEBASE Study, Frogtech Pty Ltd, Canberra, Australia.

Glover, P.W.J., 2000. Petrophysics – MSc Petroleum Geology. Department of Geology and Petroleum Geology, University of Aberdeen, UK, 376.

Harper, M., 1971. Approximate Geothermal Gradients in the North Sea Basin. Nature, vol. 230, 235–236. https://doi.org/10.1038/230235a0

Kearey, P., Brooks, M., Hill, I., 2002. An Introduction to Geophysical Exploration. Blackwell Science Ltd. Third Edition. ISBN 0-632-04929-4

Lyngsie, S.B., Thybo, H., 2007. A new tectonic model for the Laurentia–Avalonia–Baltica suture in the North Sea: a case study along MONA LISA profile 3. Tectonophysics, vol. 429, 201–227. https://doi.org/10.1016/j.tecto.2006.09.017

NSTA, 2022. UK National Data Repository (NDR). Available at: https://ndr.nstauthority.co.uk/ (Last visited October 19, 2022)

PGS, 2017. East Shetland Platform OGA 2D Interpretation Workflow Report. PGS Reservoir (for UK Oil & Gas Authority), March 2017/16.1931, available online at: www.ukoilandgasdata.com/dp/pages/apptab/ITabManager.jsp

Reynolds, J.M., 2011. An introduction to applied and environmental geophysics. John M. Reynolds – 2nd ed. Wiley-Blackwell. ISBN 978-0-471-48535-3

Scisciani, V., Patruno, S., D'Intino, N., Esestime, P., 2021. Paleozoic basin reactivation and inversion of the underexplored Northern North Sea platforms: a cross-border approach. Geological Society, London, Special Publications, vol. 494 (1): 301. http://dx.doi.org/10.1144/SP494-2020-252

Zanella, E., Coward, M.P., McGrandle, A., 2003. Crustal structure. In: The Millenium Atlas petroleum geology of the central and northern North Sea. Evans, D., Graham, C., Armour, A., and Bathurst, P. (editors and co-ordinators). The Geological Society of London. 35-43